Received: 31 January 2023 | Revised: 30 March 2023 | Accepted: 7 May 2023

DOI: 10.1002/ppap.202300016

REVIEW

PLASMA PROCESSES AND POLYMERS

Plasma polymerization of biogenic precursors

Amelia Loesch-Zhang[1] | **Andreas Geissler**[1,2] | **Markus Biesalski**[1]

[1]Macromolecular Chemistry and Paper Chemistry, Technical University Darmstadt, Darmstadt, Germany

[2]Papiertechnische Stiftung (PTS), Heidenau, Germany

Correspondence
Andreas Geissler, Macromolecular Chemistry and Paper Chemistry, Technical University Darmstadt, Peter-Gruenberg-Str. 8, Darmstadt 64287, Germany.
Email: andreas.geissler@tu-darmstadt.de

Funding information
Fachagentur Nachwachsende Rohstoffe, Grant/Award Number: 2220HV017A

Abstract

Plasma-enhanced chemical vapor deposition is a highly promising tool for coating deposition due to its versatility, tunability, low chemical consumption, and cost-effectiveness, with an increasing scope of deposition methods at both low and atmospheric pressure. Adhering to green chemistry principles, biobased precursors have recently shifted into the focus of research interests. This review gives an overview of the main biogenic substance classes that have been used for the deposition of plasma polymer coatings, including natural oils, terpenes, enzymes, and lactic acid-based precursors.

The common feature of these precursors is not only their biogenic origin, but additionally the manifold properties of the resulting plasma-deposited thin films, ranging from antimicrobial properties to tunable surface-wetting characteristics, electrical conductivity, or biodegradability. This combination of unique features makes plasma-derived polymers based on natural precursors immensely attractive for manifold applications.

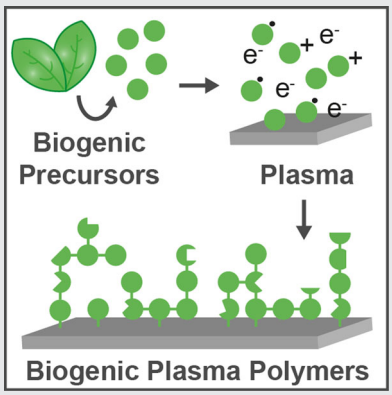

KEYWORDS

coatings, enzymes, extractives, nonthermal plasma, plasma-enhanced chemical vapor deposition (PECVD)

Abbreviations: AA-PECVD, aerosol-assisted plasma-enhanced chemical vapor deposition; ac, alternating current; AFM, atomic force microscopy; AP, atmospheric pressure; APPJ, atmospheric pressure plasma jet; CVD, chemical vapor deposition; DBD, dielectric barrier discharge; dc, direct current; MS, mass spectrometry; MW, microwave; OES, optical emission spectroscopy; PAVTD, plasma-assisted vapor thermal deposition; PECVD, plasma-enhanced chemical vapor deposition; PET, poly(ethylene terephthalate); PLA, poly(lactic acid); RF, radio frequency; ToF-SIMS, Time-of-Flight Secondary Ion Mass Spectrometry; XPS, X-ray photoelectron spectroscopy.

1 | PLASMA

The term "plasma" was first used by Langmuir et al. in the 1920s to describe the central region of an electrical gas discharge.[1] Plasma is formed when gases are supplied with such a high level of energy that their outer electrons overcome their orbital binding energy. The resulting ionized gas condition is nowadays often considered to be the fourth state of matter. It is assumed that ~99% of the universe consists of plasma.[2] In addition to stars, such as our sun, which are entirely in the state of plasma, ionized gas with much lower density also fills the space between all celestial objects.[3] Furthermore, plasma formation can be observed with *aurora borealis*, when charged particles of the solar winds interact with Earth's atmosphere and become trapped near the poles, as well as at the moment of a lightning strike.[4]

Prerequisite for plasma formation is the sufficient supply of energy to a neutral gas.[5] Methods for generating plasmas in a laboratory environment include the supply of mechanical (adiabatic compression), thermal, chemical, radiant, nuclear, or electrical energy. The most common method for producing plasmas on a lab scale is the use of electrical fields.[6] Highly energetic electrons and photons collide with neutral gas species in both elastic and inelastic collisions. Elastic collisions only change the kinetic, but not the internal energy of the neutral species. Through the inelastic collision, the electronic structure of the neutral gas particles can be modified. If the colliding electrons or photons have sufficiently high energy, electrons, ions and neutrals (atoms, molecules, and radicals) are formed in fundamental and excited states.[7,8] A plasma therefore contains free charge carriers and is electrically conductive, while at the same time showing both collective behavior and quasi-neutrality.[9]

Due to their significantly lower mass, electrons are accelerated much faster than ions or neutral gas species. This may lead to disparate temperatures for the various species contained in plasma, so that two basic types of plasma can be distinguished. Thermal plasmas, or "hot plasmas," which include solar plasma, are characterized by the kinetic energy and temperature of the heavier plasma particles reaching that of the high-energy electrons. Energy and degrees of freedom are therefore equally distributed between the particles, giving rise to the term of local thermal equilibrium (LTE) plasmas.[10,11] Opposed to this are nonthermal plasmas or "cold plasmas," also referred to as non-LTE plasmas. In this case, the electrons and part of the ions have a much higher kinetic energy than the main gas fraction. Consequently, the electron temperature (up to 10,000 K) is significantly higher than the overall gas temperature, which may well still be at room temperature. Ionization and chemical processes are therefore determined by the electron temperature. Nonthermal plasmas are less powerful but more easily controllable than thermal plasmas.[10,12] Due to their low heat generation they are well suitable for processing organic compounds.[13] Decisive for the formation of LTE and non-LTE plasmas is the efficiency of energy exchange induced by frequent collisions between electrons and heavier particles, which is enabled by a low mean free path with respect to the discharge length. High pressures and high plasma powers therefore enhance LTE plasma formation, while non-LTE plasmas are preferentially induced by lower pressures or low energy input.[14] Nevertheless, various methods exist to generate non-LTE plasmas even at atmospheric pressure.

1.1 | Plasma generation

For nonthermal plasmas, various categories exist for classification depending on their generation mechanism (direct current [dc] vs. alternating current [ac], radio frequency [RF] versus microwave frequency [MW]), pressure range (low pressure vs. atmospheric pressure) or electrode geometry.[10] Eliasson et al. suggested the categorization displayed in Figure 1, whose four main constituents will be briefly described in the following.[10] However, it should be noted that due to ongoing research in plasma generation, nowadays manifold combinations of these discharge types under varying conditions exist.[4] Nonetheless, this scheme is very useful to describe the basic functioning of these methods.

1.1.1 | Glow discharge

The term glow discharge is derived from the glow that can be observed during radiation emission of excited species that are formed in the plasma. The ions generated by inelastic collisions are accelerated toward the cathode, where an ion-induced secondary electron emission occurs on impact. The electrons released in this process can then in turn initiate further ionization. These processes of ionization and electron emission sustain the glow discharge plasma. The potential difference and resulting electric field strength are unevenly distributed in the discharge area, leading to the identification of different spatial regions (e.g., cathode dark space, negative glow, and anode zone) within the discharge. A prerequisite for sustaining dc glow discharges is the presence of two conducting electrodes. In the case of

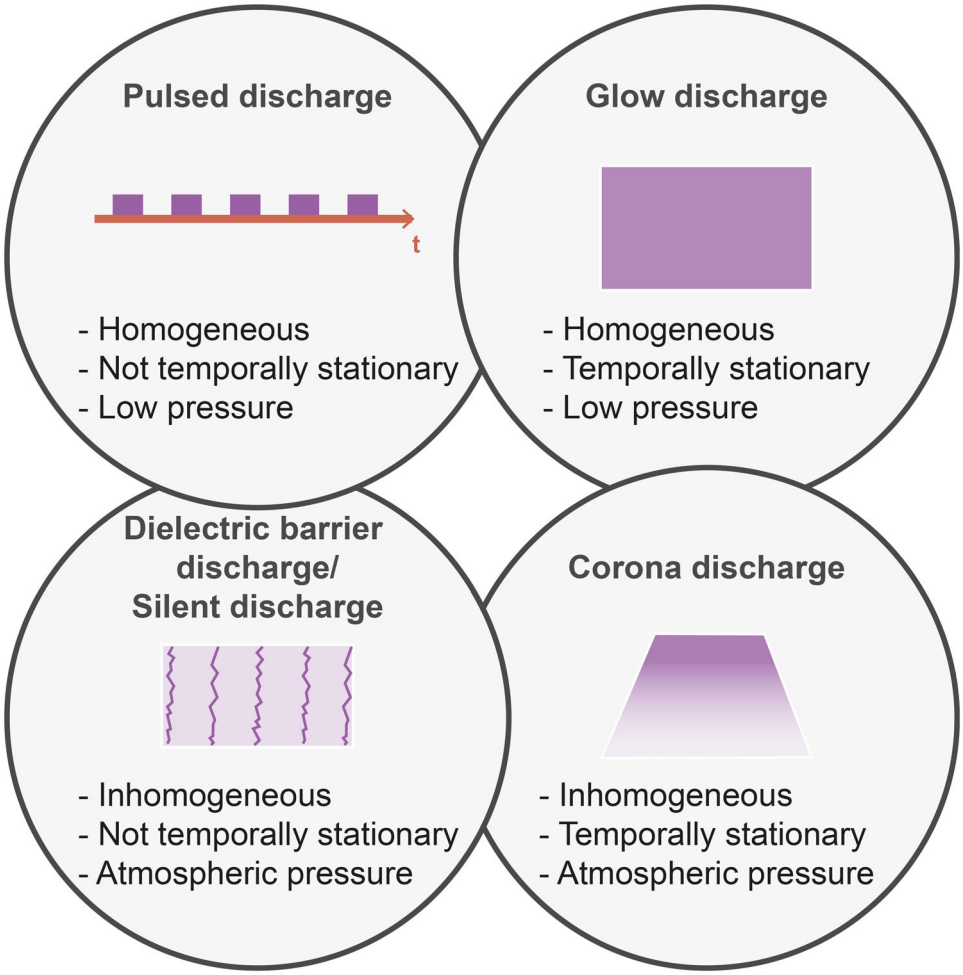

FIGURE 1 Categorization of discharge types depending on their temporal behavior, pressure, and appearance as proposed by Eliasson et al.[10]

nonconducting electrodes or in the presence of a dielectric layer, an alternating current is applied to avoid excessive electrode charging and extinction of the glow discharge. Usually, radio frequencies are used to generate alternating voltages. Pulsed glow discharges can be considered as very short dc glow discharges with a long afterglow time. They have the advantages of facilitating the generation of non-LTE plasmas and allowing higher peak voltages and currents, while achieving better efficiencies and avoiding excessive sample heating. Atmospheric pressure glow discharges face the challenge of excessive cathode and gas heating and arcing due to high pressure. This can be overcome by changing the device dimensions as well as by covering at least one of the electrodes with a dielectric and operating at alternating voltages. Operation is possible both in homogeneous and filamentary mode, respectively. Processing at atmospheric pressure is technologically less challenging than operating at vacuum conditions and allows treatment of a wider range of materials.[14]

1.1.2 | Dielectric barrier discharge

Dielectric barrier discharges (DBDs), also called "silent discharges" are very similar to atmospheric pressure glow discharges.[14] DBDs were first introduced by Siemens in 1857 for the ozonation of air.[15] DBD devices consist of two planar or cylindrical electrodes with a discharge gap width between 0.1 mm (or even smaller) and up to 100 mm. The characteristic feature is the presence of one or two insulating layers (dielectric barriers) in contact with the discharge in the gap (Figure 2a). Materials for the insulating layer include glass, quartz, ceramics as well as thin coatings from enamel or polymer on the electrode itself. For the subsequent plasma treatment, the substrate in question is placed on top of the insulation layer unless it acts itself as a dielectric layer.[16] As direct current cannot pass the insulating layer, alternating current has to be used.[17] When an electrical field is applied to a DBD device, electron avalanches develop and initiate streamers,

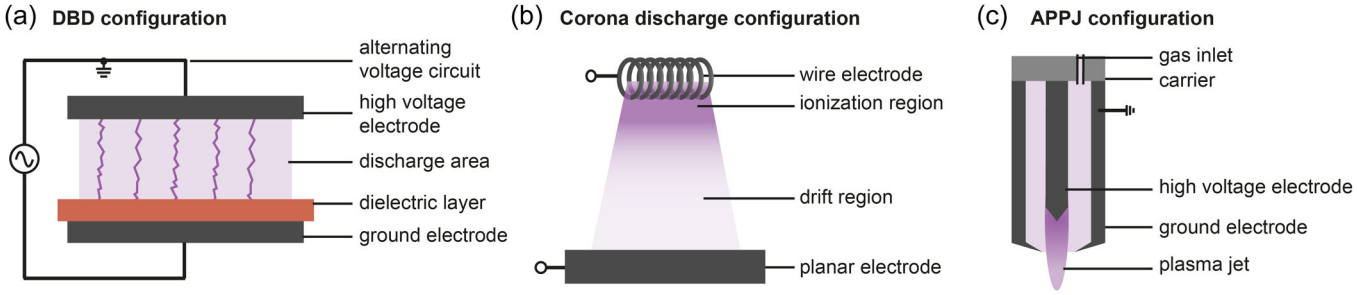

FIGURE 2 Examples of device configurations for (a) dielectric barrier discharge (DBD), (b) corona discharge, and (c) atmospheric pressure plasma jet (APPJ).

leading to the formation of a conducting channel of weakly ionized plasma and allowing the flow of an electron current.[18] Charge accumulates on the dielectric layer until the voltage polarity (and thereby anode and cathode) reverses, leading to the formation of new avalanches and streamers on that spot. These can macroscopically be observed as filament or micro-discharge.[12] Because of the charge accumulation this local electric field eventually breaks down and the micro-discharge stops.[19] The filaments formed during the discharge are nearly cylindrical plasma columns with a lifetime in the range of several nanoseconds.[20] The dielectric barrier prevents arc formation by limiting the current flow through restriction of the amount of energy in a single micro-discharge and distribution of the micro-discharges across the electrode area.[10] However, the filamentary character of the discharge makes the plasma inhomogeneous, which limits the DBD applicability in deposition and etching to smooth surfaces.[21] Under certain conditions, an alternative approach is therefore using the more homogeneous glow discharge for surface treatment or thin film deposition.[4]

1.1.3 | Corona discharge

Corona discharges differ from the previously named setups by the cathode, which is shaped like a wire, sharp tip or rough edge, while different anode geometries exist.[22] An example is given in Figure 2b. The discharge mechanism is like that of a dc glow discharge. Corona discharges operate at atmospheric pressure at dc and in nonequilibrium state in pulsed form.[14] The ionization is controlled by the electrode geometries and its zone is confined to a very small space around the cathode (ionization zone). In contrast to other plasma generation methods, there is a large low-field drift region of low conductivity between the cathode and the anode (low-field zone). The discharge is therefore highly inhomogeneous. Yet, this array stabilizes the discharge and prevents arc formation. Due to the high number of inelastic collisions occurring in the ionization zone, the species reaching the drift region have energies lower than ionization energies, so the drift region is characterized by neutral chemistry. Depending on the electrode polarity, positive and negative coronas are differentiated, although some other types also exist.[6,10,13,21]

1.1.4 | Device configurations

For industrial applications, atmospheric pressure plasmas are more suitable than low-pressure plasmas due to the simplicity of device setup, cost-effectiveness, controllability, and in-line applicability.[23] Corona discharges, atmospheric pressure glow discharges and DBD are frequently used for atmospheric pressure plasma processing.[24] The challenge of treating complex 3D objects is addressed by atmospheric pressure plasma jets (APPJ).[25] They consist of an inner needle-shaped electrode connected to the power source and a grounded outer electrode (Figure 2c). Frequently, the outer electrode is covered on the inside by an insulating layer. Carrier and reactive gases at atmospheric pressure and room temperature flow between the electrodes and become ionized. The plasma exits the device through a nozzle and is directed onto the substrate.[26] The plasma is most commonly generated via DBD, as neither corona discharges are suitable due to their discharge heterogeneity, nor glow discharges because of the low pressure required.[27] A high variety of different device setups, component materials, and potential applications exist.[20,28] The main advantages of APPJs are their ability to create a homogeneous high plasma flux and the possibility of using compact, low-cost plasma sources. A downside of this design is the pronounced point discharge characteristic which requires scanning or array mounting for treatment of larger areas.[27] As the plasma is not generated directly at the substrate surface, high processing speeds are possible, however, plasma species

can react with their surroundings on their way to the surface, causing a decrease in efficiency. The high process gas consumption, the relatively low treatable surface area and the need for cooling limits the profitability of APPJ.[29] Other setups have been recently designed to address such challenges, such as the disc jet developed by Bellmann et al.[29]

1.2 | Plasma-assisted surface processing

Plasma is an increasingly important tool for surface processing to tune chemical and physical properties of various materials ranging from metals and glasses to polymers, which this review is concerned with. An enormous range of applications from agriculture to medicine, smart surfaces, electronics, optics, and so on arises therefrom.[30,31] Depending on their impact on the substrate surface, plasma processing methods can be divided into different categories (Figure 3).

Plasma cleaning and plasma etching both refer to plasma treatment techniques in which material is removed from a substrate surface, only differing by the extent of the removal.[31,32] Plasma cleaning refers to the removal of contaminants such as oil, dust, oxides, or even bacteria from a substrate surface. Plasma etching describes the gradual removal of exposed surface layers of a bulk material. As only the material surface is exposed, the influence of etching on the physical and chemical properties of the substrate is limited, especially since UV light and the resulting radicals have a limited penetration depth.[7,33,34] Plasma etching enables for instance targeted surface roughening to generate nanostructures.[35]

Plasma functionalization or activation is used to modify substrate surface functionalities via reaction of the plasma species with the substrate surface.[36] The resulting functionalities and properties depend on the nature of the plasma, which makes this method highly useful both for tuning of surface properties and for surface pretreatment followed for instance by grafting approaches.[34,37] Typically used gases include noble gases such as Ar and He, but also O_2, N_2, NH_3, and CF_4.[37,38] For instance, an oxygen treatment leads to an increase in oxygen-containing functionalities and thereby to improved surface hydrophilicity, while hydrophobicity can be enhanced by using fluorinated compounds like CF_4 or SF_6 as reactive gas.[39] Nonreactive gases do not introduce functional groups but induce radical formation and thereby create reactive sites that can induce cross-linking (crosslinking via activated species of inert gases, CASING),[32] lead to activation or ablation, or be used for posttreatment functionalization. Upon exposure to air or oxygen, autoxidation reactions form (hydro)peroxides, which can be used for subsequent conventional grafting from polymerization.[37,40]

Alternatively, monomer adsorption to the substrate can be combined with plasma treatment if the precursor is not volatile enough to be transferred to the gas phase. In this case, the coating is performed via conventional methods, while surface binding is ensured with plasma treatment.

In the context of biogenic precursors, plasma treatment approaches have been used with copaiba oil,[41] oleic acid,[42] lavender and tea tree oil,[43] and limonene and myrcene.[44]

In the following, this review will focus on plasma polymer deposition. During plasma polymer deposition,

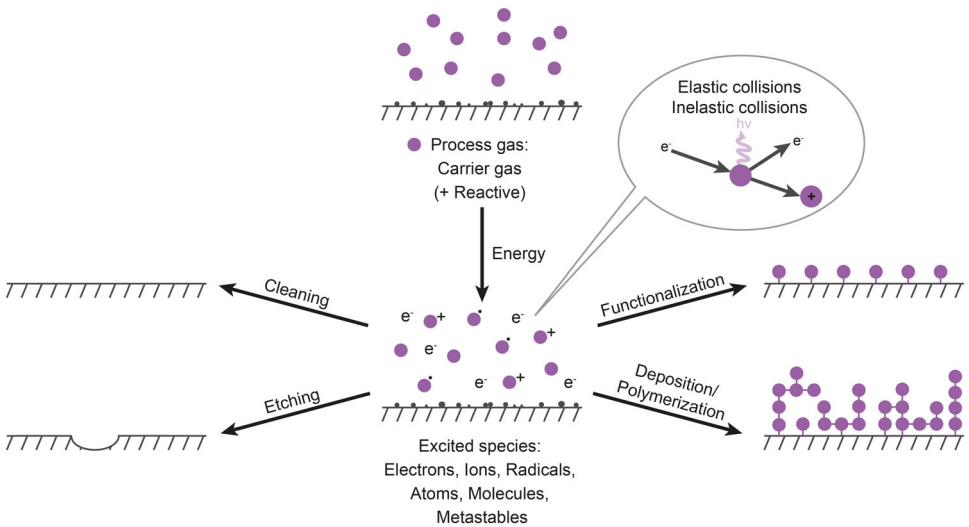

FIGURE 3 Plasma-assisted surface processing methods include plasma cleaning, etching, functionalization, and deposition.

single molecules do not only react with and attach to the substrate surface, but they also react with each other, creating an entire material layer. Plasma polymer deposition is therefore a process in which the application of a coating completely changes the surface properties while leaving the characteristics of the base material unaffected. Various methods using plasma exist, the best known among which is plasma polymerization.[34] The term is derived from the occurrence of successive plasma-activated radical initiation, propagation, and termination reactions that lead to the deposition of a polymeric coating. Contrasting with conventional polymers, plasma polymers do not comprise regular repeating units, but form irregular, highly crosslinked networks of monomer fragments.[45] Another term is "plasma-enhanced chemical vapor deposition" (PECVD). Just like in conventional chemical vapor deposition (CVD), a gaseous precursor reacts with a solid substrate surface forming a solid reaction product while simultaneously releasing gaseous byproducts.

Early research on the formation of polymeric structures in plasmas was conducted in the first half of the 20th century[46,47] and intensified starting from the 1950ies.[48–51] It was found that when gaseous compounds are subjected to plasma, insoluble solids are formed in the gas phase[47] and films can be deposited.[49] The resulting structure only partly corresponds to that of the precursor,[51] while crosslinking is usually observed. Different rates for film formation were observed for different precursors.[50] Yasuda et al. examined the effect of pulsed discharge on plasma polymer formation, showing that during plasma off-periods addition polymerization occurs exclusively, while competing with delamination processes during plasma on-periods.[52]

Due to the high energy input, the polymers formed during plasma polymerization are partially fragmented and thus deposition and ablation continuously compete with each other. The process can be tuned by many parameters, such as the nature of the plasma, the energy generation and device geometry and the deposition conditions including flow rate, use of a carrier gas, pressure, and plasma power as well as the substrate material, roughness, and temperature.[2,25,52–55] Initially plasma polymerizations were described by these partly interdependent parameters, which do not allow comparing different polymerization systems or monomers. Indeed, up to now it is difficult to reproduce plasma polymers if not exactly similar deposition conditions are used. To address these challenges, in the 1970ies Yasuda et al. developed a new parameter for describing the conditions of plasma formation, depending on (1) the power input W, which is highly dependent of the monomer chosen, (2) the monomer flow rate F, which correlates to the pressure in a closed system, and (3) the monomer molecular weight M. The W/FM parameter, or Yasuda parameter, therefore describes the energy input per mass unit of monomer transferred to the monomer molecule crossing the active plasma zone and governs the formation of reactive intermediates.[56] However, the Yasuda parameter can only be applied under limited circumstances, as it does not take into account the type of discharge, possible precursor dilution in inert gases or varying precursor reactivity.[57]

Yasuda et al. also produced important findings with respect to the mechanism of plasma polymer formation, showing that certain precursor functionalities favor decomposition, such as oxygen-containing groups, chlorine atoms, and aliphatic or cyclic hydrocarbons, while other functionalities, such as aromatics, C=C double bonds, amine, and Si-containing groups favor polymer deposition.[58] Polymerization was found to occur via radical formation, either by hydrogen abstraction or opening of multiple bonds or cyclic structures.[59]

Much further research has been conducted into the mechanism of plasma polymerization, frequently confirming these observations. Plasma fragmentation generally follows bond dissociation energies, with the weakest bonds breaking most readily.[60] Therefore, the presence of double bonds leads to increased retention of other precursor functionalities in the resulting polymer, since the π-component of C=C double bonds possesses a relatively low binding energy.[61] Using mass spectroscopy, Mertens et al. showed that the presence of double bonds leads to formation of rather large fragments and even oligomerization via double bond opening, while homologous monomers containing no double bonds show very strong fragmentation into small molecules.[53] Double bond opening has been ascribed to the formation of biradicals with a strong recombination tendency.[52,62] Nisol et al. conducted manifold investigations into the energetics and mechanistic processes of a wide range of monomers such as esters, hydrocarbons, and so on.[63] Friedrich et al. reviewed the mechanisms of plasma polymerization, identifying the main reaction pathways taking place following fragmentation such as chemical chain-growth polymerization (radical or ionic), ion-molecule reactions, and (poly-)recombination leading to linearly or irregularly structured materials and copolymers. Plasma polymerization processes performed in continuous wave mode are the least similar to conventional polymerization mechanisms and can best be described with a fragmentation-(poly)recombination mechanism. Due to the immense energy input, precursor molecules are strongly fragmented, with subsequent fragment (poly)recombination creating a structurally inhomogeneous product.[62]

For tailoring applications, retaining precursor functionalities has gained increased attention in recent years. Functional group preservation has been obtained, for instance, by maintaining a low substrate temperature, using low plasma powers, or pulsing the plasma discharges.[64]

Pulsing plasma has various advantages: The plasma can be operated at higher instantaneous power and peak voltages, while the average power is unchanged. The process can be more easily controlled and film inhomogeneity can be reduced.[5] At atmospheric pressure, the formation of thermal equilibrium, overheating, and arc/spark formation can be prevented.[7] Pulsed discharges can be produced with different device configurations and include radio frequency (RF) and microwave frequency (MW) discharges mostly operating at 13.56 MHz and 2.54 GHz respectively.[19]

The key parameter in pulsed plasma polymerizations is the duty cycle, which is defined as the plasma on-time t_{on} divided by the total pulse duration (t_{on} and plasma off-time t_{off}) (Equation 1):

$$\text{Duty cycle} = \frac{t_{on}}{t_{on} + t_{off}}. \quad (1)$$

During t_{on}, electrons, photons, radicals, ions, and metastable states are created and initiate reactions, but most of them react quickly during t_{off}. Radicals are more stable and can at atmospheric pressure induce free radical polymerization during t_{off}. Long t_{off} periods therefore result in better monomer and polymer structural retention.[65] For instance, in this way the preservation of hydroxyl-functionalities was tunable during PECVD of allyl alcohol, which allowed tailoring of surface properties.[66]

Advantages of PECVD over CVD include processing at much lower temperatures and allowing use of more sensitive precursors and substrates such as cellulose.[23,67] PECVD can be performed using low frequency, corona, DBD, radio frequency and microwave frequency plasma sources at both low and atmospheric pressure.[68] Atmospheric pressure PECVD (AP-PECVD) is gaining increasing attention as its advantages are manifold, such as the enablement of continuous processing using open systems. No expensive vacuum pumping systems are required, which reduces cost and energy consumption. A large variety of precursors are accessible. The method is suitable for homogeneous treatment of large surfaces as well as for deposition of micro- and nanoscale structures.[25,69] However, AP-PECVD also faces some downsides caused by the relatively short mean free paths and resulting high gas phase reaction rates induced by atmospheric pressure. Secondary reactions occur in the gas phase and mass transport is limited, which leads to the formation of powder contaminating the substrate surface as well as poor film uniformity and properties.[24]

AP-PECVD can be operated in direct or remote mode. In direct mode, the substrate is placed between the electrodes and the active species are created in the discharge area, leading to full precursor decomposition and requiring precise control of process parameters. In remote mode (APPJ), the precursor is injected downstream from the discharge area in the post-glow, yielding larger precursor fragments. This process extends the possible substrate selection to complex 3D substrates, but increases difficulty in achieving a uniform layer distribution.[25,68,70] Examples of AP-PECVD include deposition of silicon compounds such as hexamethyl disiloxane (HMDSO) and tetraethoxy silane (TEOS)[71] as well as deposition of fluorine compounds such as C_2F_4, C_3F_6, or C_3F_8[72] for instance with the aim of substrate hydrophobization. Another example is the use of hexamethyl disilane (HMDS) and tris(trimethoxysilyloxy)vinylsilane (TTMSVS) as antireflective coating layer for poly(ethylene terephthalate) (PET).[73] Even superconductive films have already been deposited.[74]

Plasma polymerization is also receiving great attention in the biomedical field. Tetraglyme has been deposited with an atmospheric plasma torch for obtaining protein-repellent coatings,[75] while biocompatible coatings were produced from tetraethylene glycol dimethyl ether and lactic acid.[76] Various reviews on the use of PECVD at both low and atmospheric pressure for manifold applications have been published.[69,77]

With the focus of research interests shifting toward sustainability, the implementation of green chemistry in coating strategies has become of primordial importance. PECVD is expected to play a key role because of its low coating material consumption, no solvent use, cost-effectiveness, adjustability, and possibility to apply complex multi-layered systems. Biogenic precursors are of key relevance in replacing fossil-based resources, while at the same time offering exciting new features for functional materials. Of special interest are precursors that not only occur in nature, but additionally show inherent special properties to be transferred to the coating, such as biodegradability or bioactivity. Other biogenic precursors have already been plasma polymerized for their electrical properties, making them suitable for organic electronic devices. However, the structures of biogenic precursors are often very complex, which increases the difficulty in tuning plasma deposition conditions to ensure structural and functionality retention as well as film stability to suit the desired applications. Post-deposition auto-oxidation processes must equally be taken into account concerning both short-term and long-term property analysis.

Obviously, the number of chemical substances that can be found in nature is extremely vast and greatly exceeds the scope of this work. In the following chapter, we will therefore focus on the most prominent biogenic chemical substance classes that have been plasma polymerized to obtain specific functionalities. An initial focus will be placed on essential oils, which are the first biobased precursors to have been plasma polymerized, followed by plant-based extractives such as terpenes, equally being essential oils' main constituents, which allow clear attribution of plasma polymer properties to individual chemical components. A second class of plasma polymerized materials are amino acids and enzymes. Here, the preservation of the required bioactive center is especially challenging. Finally, the plasma polymerization of lactic acid and its derivatives is reviewed, as these polymers are of interest due to expected ease of biodegradability.

FIGURE 4 Examples of plants serving as sources for essential oils that have already been used for plasma polymerization.

2 | PECVD OF BIOGENIC PRECURSORS

2.1 | PECVD of essential oils

Essential oils, formed as secondary metabolites by many plants, have been extracted from natural compounds for centuries and used for example for their antiseptic properties as well as their fragrance. In modern industry, they are used in cosmetics, sanitary and medical products as well as in agriculture and food industry.[78–80] While about 3000 different essential oils are known, only 10% are of commercial relevance. Essential oils are mixtures of about 20–60 different components, with the main groups being (1) terpenes and terpenoids as well as (2) aromatics and aliphatics, which all possess different biological properties.[78–80] In nature, essential oils protect plants against bacteria, viruses, fungi, insects, and herbivores. They are easily available from biological sources, at low cost and in commercial quantities. On the other hand, they show very low human toxicity (i.e., harmful potential for humans).[78–80] These factors make essential oils very interesting starting materials for new "green" functional coatings, as can be obtained through plasma polymerization (Figure 4).

The first to plasma polymerize essential oils were Sakthi Kumar et al., using **lemongrass oil** and **eucalyptus oil**. Polymerization was performed at radio frequency under reduced pressure to obtain metal-insulator-metal structures and analytics were focused on the electrical properties and conduction mechanism of the resulting thin films, which was found to be of the Schottky type in both cases.[81,82] The eucalyptus oil plasma polymer was further examined after deposition on glass substrates using IR spectroscopy where reduction or lack of C–H and C–C bending modes indicated the formation of highly crosslinked structures. The optical band gap was found to be at 1.53 eV.[82]

Jacob et al. initiated a wide range of investigations on the plasma polymerization of essential oils at RF power and reduced pressure with the goal of obtaining new materials for organic electronical and optical applications by plasma polymerizing **lavender oil**. Deposition times of 5–90 min at 25 W RF power enabled the preparation of transparent, very smooth films with thicknesses in the range of 200–2400 nm characterized by an energy gap of 2.93 eV, a refractive index of 1.565 (500 nm) and an extinction coefficient of 0.01 (500 nm).[83]

Extensive research on plasma polymerized thin films from lavender oil was continued by Easton et al., wherein the influence of plasma power on the resulting films was examined. The films were deposited on precleaned glass substrates in a glow discharge at reduced pressure and at RF plasma powers ranging from 10 to 75 W. The retention of the precursor structure, especially of C=C double bonds, decreased with plasma power, while fragmentation increased.[84] Except for the optical band gap, which was slightly higher than that observed by Jacob et al., optical parameters were found to be independent from the plasma power.[85] Solubility tests showed the plasma polymer's insolubility in various solvents. Water contact angles ranged between 82° and 91° increasing with RF power.[86] Aging effects were associated to oxidation and etching processes.[87]

Al-Jumaili et al. examined the properties of plasma polymerized **geranium oil** thin films as a function of plasma power. Refractive index, extinction coefficient, and optical band gap were generally independent from the plasma power, while the surface roughness, hardness, elastic modulus, wettability, and solubility resistance increased with plasma power. A higher degree of crosslinking resulting from higher plasma powers impedes the reorientation of functionalities at the interface and increases the film rigidity, resulting in more stable contact angles over time. The authors examined the biofilm formation of *Staphylococcus aureus, Pseudomonas aeruginosa, and Escherichia coli* on films deposited at 10 and 50 W. Decreased bacterial attachment and biofilm formation on plasma polymer films deposited at 10 W as opposed to those deposited at 50 W was attributed to the combined effects of retention of the structural integrity of the bioactive precursor, surface morphology and chemistry (especially the presence of hydroxyl groups).[88] Electrical properties were investigated by incorporating plasma polymer thin films derived from geranium oil into metal-insulator-metal sandwich structures with aluminum electrodes. The conductivity values were typical for insulating materials. The optical band gap decreased slightly from 3.67 to 3.60 eV for higher plasma powers, which was explained by the increased presence of dangling chains that might lead to formation of additional intermediate energy levels and/or defects decreasing the optical band gap.[89]

Hennekam et al. analyzed the fragmentation occurring in the plasma phase during PECVD of **sandalwood oil** at reduced pressure and 2–50 W RF power. The gas phase was characterized using mass spectrometry (MS) and optical emission spectroscopy (OES), while the resulting films were characterized with X-ray photoelectron spectroscopy (XPS), Time-of-flight Secondary Ion MS (ToF-SIMS) and atomic force microscopy (AFM). Oligomers were formed at low plasma powers, with a relatively good stability being assigned to the bridged cyclic ring structure of santalol. With increasing RF power, hydrogen abstraction, and crosslinking were enhanced, while the incorporation of oxygen-containing groups was reduced. At the same time, an increased formation of smaller fragments was observed, which were detected for example in the form of carbon monoxide and ethylene in the plasma.[90]

Mol et al. examined the optical absorption and emission properties of plasma polymer films made from **tea tree oil**. Depending on the irradiation wavelength, photoluminescence emissions occurred in the yellow spectral region (465–695 nm) and IR region (850–1090 nm) and were attributed to the presence of chromophore units and polaronic transitions as well as interchain emission respectively. UV-Vis absorption signals at 332 and 558 nm were attributed to C=O groups inducing π–π^*-transitions of the aromatic ring as well as interchain π–π stacking interactions respectively. IR spectroscopy showed that band maxima shifted depending on the substrate used, indicating a variation in bond lengths depending on the substrate and showing that amorphous glass substrates are better scaffolds for plasma polymer growth than crystalline silicon substrates.[91] Bazaka et al. were the first to examine the effects of plasma treatment with Ar APPJ on thin films from tea tree oil plasma polymers upon PET substrates. Compared to as-deposited plasma polymers, APPJ-treated plasma polymers showed increased surface oxidation, with three potential oxygen sources being: fragments of oxygen moieties from retained precursor molecules, coating exposure to ambient air and reactions between Ar plasma and ambient air. Slight changes in surface roughness were observed and primarily attributed to the removal of loosely attached low molecular weight fragments by the plasma. Contact angles decreased nonlinearly with plasma treatment from >70° to ~57° after 5 s and <40° after 60 s due to surface oxidation. The bioactivity against *S. aureus* was partially and temporarily improved due to easy release of antimicrobial low molecular weight fragments.[92] Jacob et al. are among the researchers using PECVD for deposition of graphene from natural substances, focusing on tea tree oil as a carbon source. They produced multilayered graphene by introducing volatile tea tree oil vapors into an H_2 gas-filled plasma chamber, inside which precursor dissociation and deposition occurred at 0.2 mbar, 800°C and 500 W RF power. The resulting films were nearly free of structural defects and mainly consisted of sp^2- and some sp^3-hybridized C atoms as well as some C–O bonds. The contact angle was 135° due to combined effects of material hydrophobicity and nanoscale surface morphology. Suitable electrical properties also showed the possibility to use the films as functional component in memristors.[93]

Romo-Rico et al. compared plasma polymerization of **oregano oil** onto glass slides at reduced pressure in continuous wave and pulsed mode. Water contact angles of 45° and 7° were obtained respectively. The plasma polymers showed antibacterial activity against *S. aureus* and *P. aeruginosa* whilst supporting human dermal fibroplast adhesion.[94]

Considering essential oil-based plasma polymers, it is important to remember that essential oils are natural products whose composition may vary from batch to batch. Results from different research works can therefore not be easily compared and may not always be entirely reproducible with materials from different suppliers or batches.

Table 1 gives an overview of frequently analyzed parameters of plasma polymerized essential oils.

TABLE 1 Plasma polymerized essential oils and commonly analyzed properties.

	Optical properties			Surface properties		Mechanical properties		Electrical properties				
Precursor	**Refractive index**	**Band gap (eV)**	**Extinction coefficient**	**Roughness average (nm)**	**Roughness RMS (nm)**	**Hardness (GPa)**	**Elastic modulus (GPa)**	**Dielectric constant**	**Conductivity ($\Omega^{-1}m^{-1}$)**	**Water contact angle (°)**	**Antimicrobial properties**	**Literature**
Eucalyptus oil	1.55	3.66; 1.53	0.006	-	0.2	-	-	-	-	-	-	[82, 95]
Geranium oil	-	3.67–3.60	-	0.23–0.60	0.30–0.77	0.63–0.85	9.39–20.61	4.40–2.10	10^{-16}–10^{-17}	54.0–65.6	*Staphylococcus aureus, Escherichia coli, Pseudomonas aeruginosa*	[88, 89]
Lavender oil	1.53–1.57	2.93–2.34	0.001	0.41–0.37	-	-	-	-	-	81–92	-	[83–85]
Orange oil	1.55	3.60	-	0.62–1.14	0.79–1.51	0.50–0.78	-	-	-	-	-	[96]
Oregano oil	-	-	-	-	-	-	-	-	-	45°/7°	*S. aureus, P. aeruginosa*	[94]
Sandalwood oil	-	-	-	-	1.35–0.64	-	-	-	-	-	-	[90]
Tea tree oil	-	3.19	-	-	-	-	-	-	-	-	*S. aureus*	[91, 92, 97]

Note: For detailed results and deposition conditions, please be referred to the cited literature.

2.2 | PECVD of extractives

In contrast to the use of essential oils, the functionality and structure of plasma polymer thin films obtained from pure extractives can be attributed to defined precursor molecular patterns. Extensive research has been performed on the plasma polymerization of terpenes (Figure 5), which constitute 90% of the components in essential oils, and many of which are known to be antimicrobial agents.[78,80] They can be extracted from crude essential oils and are therefore relatively easily accessible.

Very early research was performed by Linder et al. in 1931, who examined the effect of a glow discharge on 57 different hydrocarbons in the gas phase, amongst them being the terpenes limonene and pinene. Analysis of the evolution of the formation of gaseous and solid species and their chemical composition showed very similar gas compositions regardless of the original feedstock. The comparatively high amount of unsaturated species contained in most of the formed gases was attributed to relatively mild discharge conditions compared to other works of the time.[47]

Bazaka et al. plasma polymerized **terpinen-4-ol**, a key component of tea tree oil, using a glow discharge device with RF power at reduced pressure. In agreement with comparable studies, the film thickness was found to increase with deposition time.[98] Continuing these investigations, Kumar et al. found that the chemical structure of the films depends on the substrate temperature, because it affects the balance between adsorption and desorption on the surface, leading to the formation of different chemical functionalities and surface morphologies.[99]

The fragmentation behavior of terpinen-4-ol in plasma was examined by Grant et al. using residual gas analysis and positive ion mode mass spectroscopy. Both techniques showed precursor fragmentation to increase with RF power, with a significant amount of precursor being retained at relatively low plasma power up to 10 W (Figure 6).[97]

Accordingly, the optical, physical, and chemical properties of terpinen-4-ol thin films, such as optical band gap, refractive index, extinction coefficient, hardness, chemical stability and contact angle, are tunable with plasma power. Films deposited at higher RF power showed a surface with more, narrower and sharper peaks, while there was no significant change in surface roughness parameters R_a, R_q, and R_{max}.[55] AFM further showed the surface to be smooth and pinhole-free, indicating the polymerization to have occurred directly on the substrate surface and not in the gas phase, which would result in "dust" on the surface.[98]

Samples were stored in ambient conditions for almost 50 days to examine the effects of aging. Refractive index measurements showed the main material property degradation to take place within the first week after deposition. Its origin was found in oxidation processes as well as volumetric relaxation in the material.[100] Due to their relatively good retention of the precursor chemistry during the deposition process, films deposited at 10 W showed antimicrobial properties against *S. aureus* and *P. aeruginosa*, contrary to those deposited at higher plasma power.[101] Kumar et al. were additionally able to demonstrate antifouling properties of these coatings in the marine environment for a limited period of 1 week.[102] Jacob et al. examined the suitability of terpinen-4-ol thin films for use in flexible organic electronics by incorporating them as insulating layer in metal-insulator-metal structures and organic field-effect transistors.[103] In this context, the films' ability to simultaneously block the transport of electrons and enable the transport of holes, which is of interest for organic light-emitting diode applications, was demonstrated.[104]

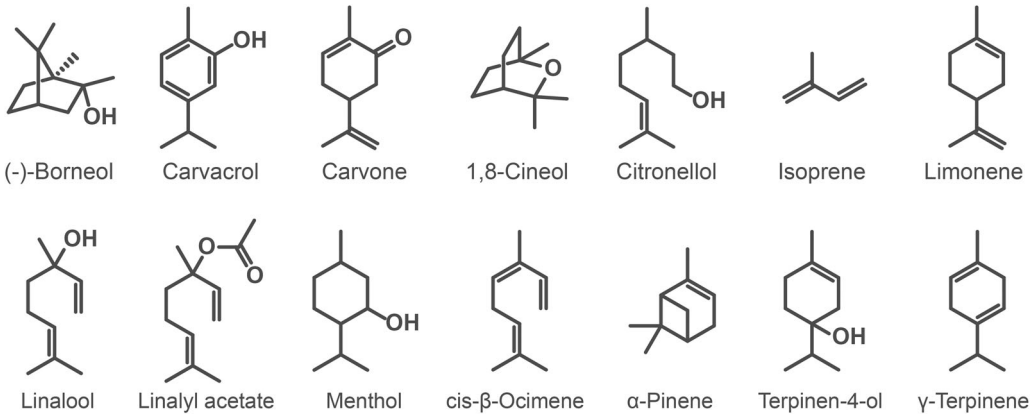

FIGURE 5 Examples of terpenes deposited via plasma-enhanced chemical vapor deposition.

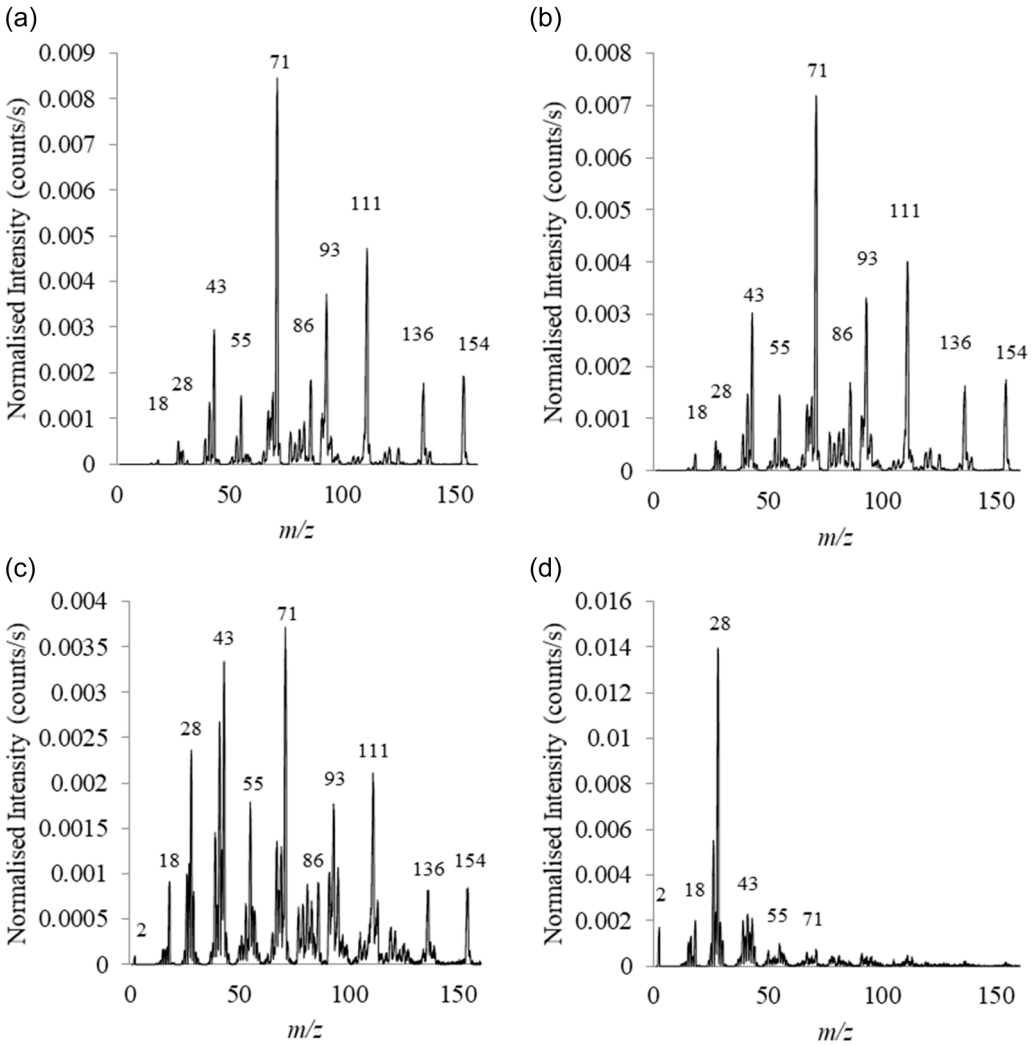

FIGURE 6 Electron impact ionization residual gas analysis mass spectra of (a) neutral terpinen-4-ol species and the plasma phase at (b) 5 W, (c) 25 W, and (d) 50 W show increased fragmentation for higher plasma powers, the peak at $m/z = 154$ representing the terpinen-4-ol monomer.[97] Reproduced from Grant et al.[97] (CC BY 4.0). Copyright 2021 by the authors.

While continuous wave deposition had been used previously for producing films from terpinen-4-ol, Kumar et al. used pulsed plasma deposition to decrease precursor fragmentation and functionality loss with the aim of retaining the precursor's antimicrobial activity. To this end, plasma polymers were deposited at a peak power of 10 W and four different duty cycles (10%, 20%, 40%, 100%, resulting in effective plasma power of 1 W, 2 W, 4 W, and 10 W) and a total deposition time of 15 min at reduced pressure with a pulse repetition frequency of 500 Hz. Chemical radical chain reactions were found to dominate at lower duty cycles and plasma polymerization at higher duty cycles. As a result, films deposited at higher duty cycles showed a higher degree of precursor fragmentation and crosslinking, making them more stable in contact with water. Both the highest bacterial attachment of *P. aeruginosa* due to the highest hydrophobicity as well as the highest antimicrobial activity were detected on films deposited at 40% duty cycle.[105]

A far more mechanistic approach was chosen by Ahmad et al., in which the fragmentation and oligomerization behavior of **γ-terpinene** during plasma polymerization was analyzed by gas phase MS. Precursor fragmentation was augmented with increasing plasma power, as shown by the decrease in higher molecular weight fraction peak intensities and increase in lower molecular weight fraction peak intensities. It is interesting to note that oligomeric species $[M + H]^+$ and $[2M + H]^+$ (M being the precursor molecule) were observed, with equally decreasing intensity at increasing plasma power. Ion deposition was an important part of film formation at all plasma powers, but a small amount of unfragmented precursor was also incorporated. The authors identified a

number of fragments and suggested fragmentation pathways (Figure 7).[106]

To evaluate the suitability of plasma polymers from plant-derived secondary metabolites as encapsulation materials for organic photovoltaics, γ-terpinene was plasma polymerized at different deposition rates onto glass substrates and onto organic solar cells, respectively, followed by investigation of the stability of the resulting films under UV irradiation. Encapsulation of the solar cell with plasma-deposited γ-terpinene led to a significantly slower decrease in device efficiency. UV irradiation-induced degradation of the plasma polymer thin films manifested itself in photooxidation of the films with the degradation pathway and velocity depending on the UV light wavelength and dose.[107]

Getnet et al. examined the suitability of **carvacrol**-based plasma polymers deposited in atmospheric pressure dielectric barrier discharge as antimicrobial coatings for stainless steel, which is frequently used as an implant and prosthetics material in underdeveloped countries. They observed antibacterial activity against *E. coli*, *S. aureus*, *P. aeruginosa*, and *C. albicans*. Good antimicrobial activity was attributed to high hydroxyl content, surface roughness, and hydrophilicity. The coatings were further stable under UV light irradiation for 1 h and to air exposure for 120 days and reduced the corrosion rate of the underlying steel substrate.[108,109]

Antibacterial properties of **1,8-cineole** plasma polymer films deposited at reduced pressure and 20 W RF power were examined by Pegalajar-Jurado et al. *S. aureus* and *E. coli* attachment to 1,8-cineole plasma polymer coated glass slides were reduced by 63% and 98% respectively compared to hydrophilic glass slides. No leaching of bioactive substances from the films into the media was observed. Preliminary experiments also indicated that neither the plasma polymer films nor potential leachables were harmful to mammalian cells.[110]

Mann et al. closely correlated surface properties and antibacterial activity of plasma polymerized 1,8-cineole films while varying plasma power (50−150 W) and pressure (15−100 mTorr). The plasma phase was analyzed with OES, while the film surface chemistry was examined with XPS and IR spectroscopy. Increasing pressure leads to less oxygen incorporation in form of alcohol/ether/carbonyl functionalities. Water contact angles correspondingly ranged from $(54.3 \pm 4.1)°$ to $(85.6 \pm 1.1)°$. Bacterial attachment assays showed decreased bacterial attachment and growth for *E. coli* after 24 h incubation and 5-day incubation compared to reference samples (Figure 8).[111]

By plasma polymerization of **carvone**, Chan et al. deposited films with an average surface roughness R_a of 0.11 nm and a water contact angle of 78.8° on glass substrates. IR spectroscopy indicated that the ring structure of the precursor was destroyed by fragmentation. Bacterial adherence of *E. coli* and *S. aureus* was decreased compared to untreated glass coverslips, along with bacterial growth which was reduced by over 80%. No cytotoxicity toward human cells was observed.[112]

Tone et al. compared the suitability of different plasma polymerized terpenes, namely **L-menthol, (S)-(-)-β-citronellol, (1S)-(-)-borneol**, and **R-limonene** for ultrafiltration membranes made from cellulose acetate for separation of racemic amino acids. They found that the coating deposition not only depends on deposition time, but also on the precursor structure and reactivity, with ring tension and double bonds leading to increased deposition rates. All membranes showed similar partition coefficients toward separation of racemic amino acid mixtures. When comparing membranes with the same degree of coating fixation at the same volume flux, those with citronellol-based coatings showed the highest separation factor.[113]

Research toward production of synthetic rubber thin films has been performed by Gürsoy et al. by plasma polymerizing **isoprene** at reduced pressure and 5–35 W RF power. The characterization of the obtained films showed a basically good preservation of the precursor structure together with a decrease of the C=C double bond content. The stretching resistance of plasma polymerized isoprene deposited on an elastomer was evaluated using contact angle measurements and the material was shown to withstand up to 1000 stretching cycles of 25% elongation and showed only small contact angle decreases at 125% elongation. Plasma polymerized

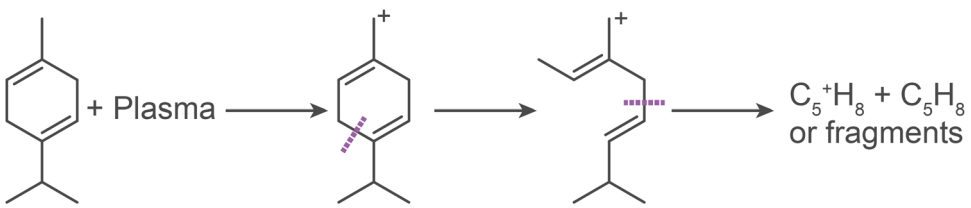

FIGURE 7 One exemplary step of the fragmentation pathway for γ-terpinene during plasma polymerization as suggested by Ahmad et al. Reproduced and adapted with permission from Ahmad et al.[106] © 2015 WILEY-VCH Verlag GmbH & Co. KGaA, Weinheim.

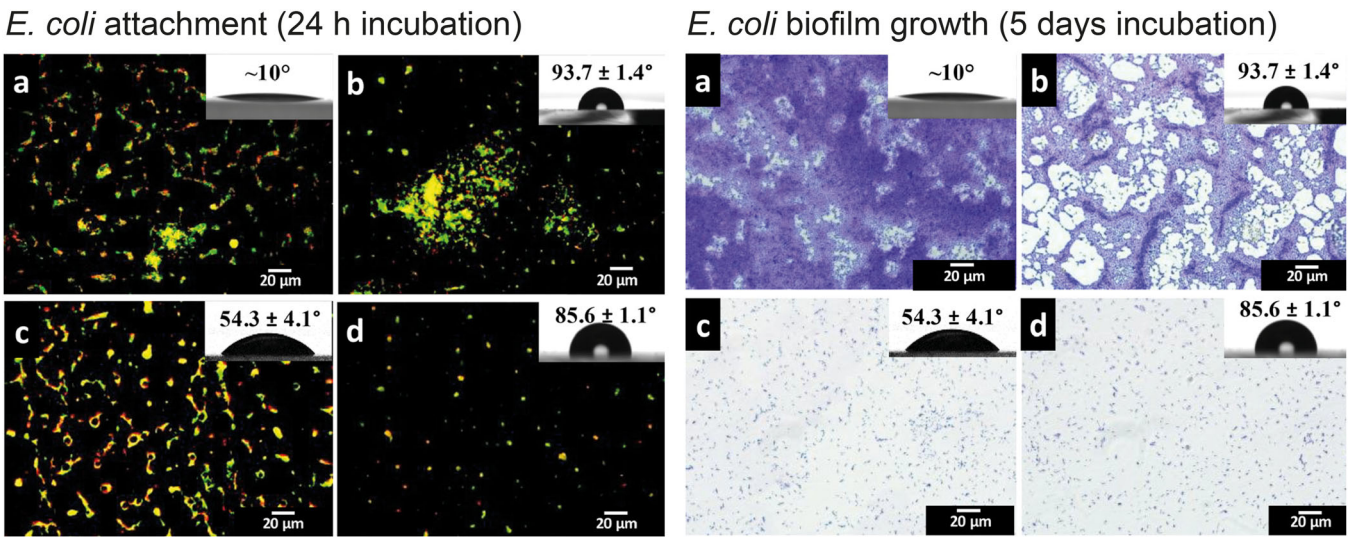

FIGURE 8 Fluorescence microscopy images (left, viable attached bacteria depicted in green, dead ones in red) and bright field microscopy images (right, samples stained with crystal violet) presented by Mann et al. show the attachment of *Escherichia coli* after 24 h and 5 days respectively on (a) control glass slides, (b) reference glass slides coated with plasma polymerized 1,8-octadiene, (c, d) plasma polymerized 1,8-cineole (low and high pressure and plasma power). Adapted with permission from Mann and Fisher.[111] Copyright 2017 American Chemical Society.

isoprene deposited on bamboo fibers showed contact angles of up to 146.8° that could be maintained after three washing cycles with liquid detergent for 30 min each.[114]

Further terpenes that have been used for plasma deposition are linalool,[115] cis-β-ocimene,[116] D-limonene,[117] and linalyl acetate.[118] Table 2 presents an overview of plasma polymerized terpenes and their commonly examined properties.

To the best of our knowledge, the only nonterpene extractive that has been plasma polymerized so far is **eugenol**. In line with their research of antimicrobial coatings based on carvacrol for steel-based implants, Getnet et al. plasma polymerized eugenol on a stainless steel substrate in an atmospheric pressure dielectric barrier discharge at effective discharge powers of around 1.2 W. At these conditions, the electron temperature was 1.5 eV assuming LTE. Initially, the film thickness increased with the applied voltage until ablation processes eventually dominated over deposition. No significant precursor fragmentation was observed in OES. IR spectroscopy of the plasma polymer film revealed that the aromatic and hydroxyl functions were retained, but the vinyl groups disappeared, and ketone groups were formed, the latter possibly due to oxidation processes after deposition. By means of IR spectroscopy, it was further demonstrated that the films are resistant to aging for 120 days in air and under UV irradiation. *S. aureus* and *E. coli* adhesion was reduced by 78% and 65% on these surfaces.[125] Antibacterial properties were equally observed for *P. aeruginosa* and *C. albicans*, as were anticorrosive effects.[109]

2.3 | PECVD of amino acids

Contrary to essential oils, which only occur in plants, amino acids can be found in all living beings. Apart from plasma-assisted two-step functionalization approaches in which suitable anchor groups are first placed on the surface and the amino acids are subsequently grafted on, direct deposition is possible, even if it results in less defined layers. Alongside some work that has used sputtering techniques for direct deposition of amino acids,[126] PECVD of histidine and tyrosine has already been described.

For biometallization, Anderson et al. used PECVD to deposit coatings from **tyrosine** on silicon wafers, PET, and cellulose nitrate substrates. Tyrosine was chosen for its ability to reduce noble metal nanoparticles such as gold from solution and bind them onto surfaces. The precursor was transferred into the gas phase via sublimation at up to 300°C in the PECVD chamber at reduced pressure followed by deposition at 60 W RF power. The obtained plasma polymer films were optically transparent in the visible wavelength range, resistant to mechanical stress and tolerated immersion in the aqueous gold chloride solution. IR spectroscopy confirmed crosslinking with high retention of tyrosine monomer functionality required for gold reduction. The

TABLE 2 Plasma polymerized terpenes and commonly analyzed properties.

	Optical properties			Surface properties		Mechanical properties		Electrical properties				
Precursor	**Refractive index**	**Band gap (eV)**	**Extinction coefficient**	**Rougness average (nm)**	**Roughness RMS (nm)**	**Hardness (GPa)**	**Elastic modulus (GPa)**	**Dielectric constant**	**Conductivity ($\Omega^{-1}m^{-1}$)**	**Water contact angle (°)**	**Antimicrobial properties**	**Literature**
1,8-Cineole	1.543	2.83	0.001	0.39	≤50	-	-	-	-	77–90	*Escherichia coli, Staphylococcus aureus*	[110, 111, 119]
Carvacrol	-	-	-	200–800	-	-	-	-	-	25–55	*E. coli, S. aureus. Pseudomonas aeruginosa, Candida albicans*	[108, 109]
Carvone	-	-	-	0.11	0.14	-	-	-	-	78.8	*E. coli, S. aureus*	[112]
Cis-β-ocimene	1.58	2.85	-	-	<1	-	-	3.5–3.6	10^{-12}–10^{-11}	94.14	-	[116, 120]
Limonene	-	-	-	0.48	-	-	-	-	-	-	-	[117]
Linalool	1.55	2.64–2.82	0.001	0.44	-	-	-	-	-	76–80	-	[115, 121]
Linalyl acetate	ca. 1.56	2.95–3.02	-	0.19–0.21	-	0.30–0.44	-	2.39–2.43; 3–3.5	10^{-11}	85.7	-	[118, 120, 122]
Terpinen-4-ol	1.55	2.67	0.0007	0.33–0.44	0.42–0.56	0.33–0.51	-	3.4	-	63–69	*P. aeruginosa, S. aureus*	[55, 98, 100, 101, 103, 123]
γ-Terpinene	1.57–1.58	3	-	0.21–0.30	0.30–0.39	0.40–0.58	4.22–5.69	3.24–3.69	10^{-13}–10^{-12}	61–81	-	[124]

Note: For detailed results and deposition conditions, please refer to the cited literature.

deposition of a patterned tyrosine PECVD coating was achieved successfully as well and enabled the selective growth of gold nanoparticles on the substrate surface.[127] Tyrosine was also used to investigate the plasma "copolymerization" of amino acids with other organic and inorganic monomers frequently used in synthetic materials, showing the possibility to obtain biologically active coatings by incorporating biomolecules into organic or inorganic matrices with the help of plasma deposition methods.[128]

Histidine was plasma polymerized by Anderson et al. onto single crystal Si wafers and 3D substrates as a precursor for enabling titania reduction and nanoparticle growth directly on the substrate. Histidine was transferred into the gas phase by sublimation at 200°C at reduced pressure, followed by plasma deposition at 50 W RF power. Immersion of the resulting film in water lead to partial dissolution, whilst the remainder of the coating was sufficient for titania reduction. IR spectroscopy showed sufficient monomer structure retention to enable titania nanoparticle formation. The latter was successful on Si wafers with a surface coverage of ~75% as well as on 3D substrates, indicating a potential use in tailoring photonic structures and creating hybrid organic-inorganic multilayer systems with highly varying refractive indexes.[129]

2.4 | PECVD of proteins

When it comes to the matter of functionality retention across the plasma polymerization process, there is one class of biogenic substances posing even more challenges that those discussed previously: Proteins and enzymes are biological macromolecules consisting of amino acids linked by peptide bonds which possess highly specific functionalities closely linked to their structure. This leads to the double challenge of not only preserving functional groups, but also the bonding sites and cavities linked to biological functionality.

Heyse et al. investigated the deposition of sprayed liquid precursors at very mild plasma conditions and atmospheric pressure to obtain maximum retention of the precursor structure and functionality for protein plasma deposition.[130] By dissolving the precursors in an aqueous carrier solution followed by atomization, they were able to deposit precursors within a polymer matrix produced by the carrier gas (C_2H_2 or pyrrole), a method referred to as aerosol-assisted PECVD (AA-PECVD) (Figure 9). The water shell formed around the precursors makes the droplets act as shuttles while serving as protection against reactions with the plasma. This enables deposition of intact proteins within the growing polymer network, and for enzymes additionally preserves their catalytic activity.[131]

Using this method, the authors were the first who immobilized proteins in organic coatings in a single-step procedure, by simultaneously polymerizing proteins and acetylene in an atmospheric pressure dielectric barrier discharge. They used fluorescein-isothiocyanate labeled **bovine serum albumin** (BSA-FTIC) and **allophycocyanin**, an auto-fluorescent protein found in cyanobacteria and red algae. Confocal and fluorescence microscopy proved a homogeneous fluorescence distribution, contrary to aggregate formation observed by conventional protein immobilization procedures. The autofluorescence of allophycocyanin further enabled proving successful intact molecule entrapment as its fluorescence emission is strongly dependent on retention of its quarternary structure (Figure 10).[132] Apart from the allophycocyanin protein, the authors further deposited **glucose oxidase, lipase**, and **alkaline phosphatase** enzymes using plasma.[131]

Alkaline phosphatase was also embedded into plasma polymer matrices from acetylene and pyrrole by Ortore et al., using an enzyme buffer solution aerosol and

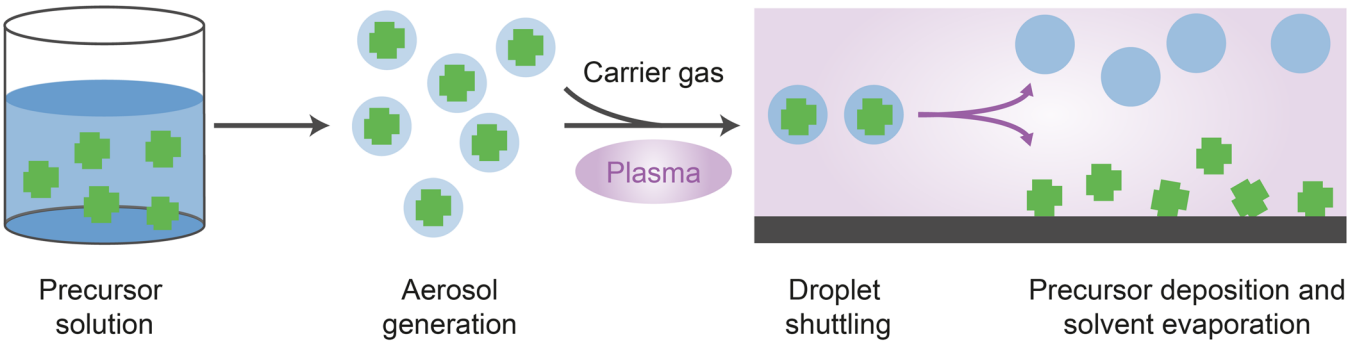

FIGURE 9 Illustration of the principle of aerosol-assisted plasma-enhanced chemical vapor deposition showing the water droplets functioning as shuttles protecting the proteins during plasma deposition.

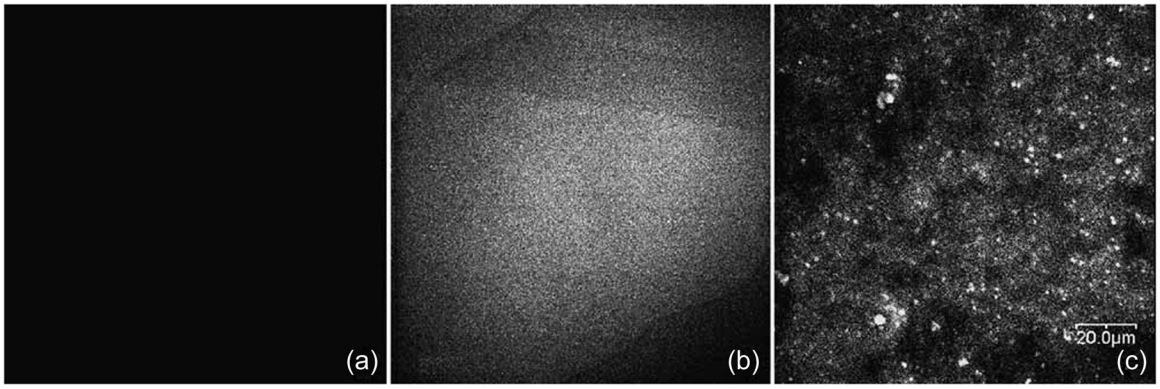

FIGURE 10 Fluorescence microscopy images prove the preservation of the fluorescent structure of BSA-FITC after plasma deposition by showing (a) pure plasma polymerized acetylene coating, (b) plasma polymerized BSA-FITC with acetylene, and (c) covalently immobilized BSA-FITC on glass as reference. Reproduced with permission from Heyse et al.[132] © 2008 WILEY-VCH Verlag GmbH & Co. KGaA, Weinheim.

atmospheric pressure DBD plasma polymerization. Grazing-incidence small X-ray scattering (GISAXS) was established as a new method to analyze the scattering patterns of the plasma polymer taking into account the various contributions from the polymer matrix and the embedded enzyme. This new technique enabled proving the protein incorporation and determining their concentration as well as the microdomain size.[133]

Palumbo et al. used the AA-PECVD technique to deposit films consisting of a plasma polymerized ethylene matrix with incorporated aqueous **lysozyme** solution using a DBD reactor. The authors were the first to examine the integrity of the embedded enzymes and the potential damage occurring during plasma deposition using Matrix-Assisted Laser Desorption/Ionization Time-of-Flight (MALDI-ToF), using α-cyano-4-hydroxycinnamic acid as matrix, and high-pressure liquid chromatography (HPLC) release monitoring. Both analytical methods indicated the absence of smaller peptide/protein fractions, meaning no substantial damage took place during plasma polymerization. The peaks for the intact lysozyme molecule were present, although somewhat widened compared to the reference, indicating that on individual lysozyme amino acids some limited degradation or modification reactions occurred in the plasma phase. The retention of the lysozyme biological activity could nevertheless be confirmed by the agar diffusion test. The release from the coating into water was found to occur within 1 day, making the material interesting for applications in drug delivery.[134]

The principle of AA-PECVD was combined with an APPJ producing corona discharge by Malinowski et al. to deposit **laccase**, an oxidoreductase enzyme forming part of the biosynthesis in plants, insects, fungi, and bacteria. Bioactivity was found to be retained to a greater extent than in coatings deposited by conventional methods, due to monomer crosslinking and covalent binding to the glass surface. Reduction of bioactivity compared to the untreated laccase enzyme was attributed to the fragmentation of monomers during the plasma process. It was found that reactions with the plasma mainly occur in the outer region of the protein while the center of the molecule remains unaffected.[135] The applicability of this method for producing laccase-based biosensors from corona discharge was found to be promising, as it could greatly decrease biosensor construction times compared to conventional methods while maintaining comparability of analytical parameters.[136] The authors further examined the binding mechanism of laccase during corona jet plasma deposition onto graphene. They demonstrated that laccase is both polymerized and simultaneously bound to solid substrates. Preservation of the molecule's active center allowed the coating to retain its bioactivity.[137]

Further enzymes and proteins polymerized via AA-PECVD in DBD include **lipase**,[138] **elastin**,[139] and **collagen**.[140,141] An overview of plasma polymerization of proteins and enzymes is given in Table 3.

2.5 | PECVD of lactic acid-based precursors

Besides the large groups of essential oils and their components as well as proteins and their components, there is a great variety of other biogenic molecules that have been used for plasma polymerization, which cannot all be cited here. The most prominent group, and therefore the only one that we will focus on, is certainly that of lactic acid and its derivatives. Poly(lactic acid) has

TABLE 3 Plasma-polymerized proteins and (potential) applications thereof.

Precursor	Deposition device	Carrier gas/matrix gas	(Potential) Applications	Literature
Alkaline phosphatase	Dielectric barrier discharge (DBD)	He/Acetylene, pyrrol	Analytics	[133]
Allophycocyanine	DBD	He/Acetylene	Protein immobilization	[132]
BSA	DBD	He/Acetylene	Protein immobilization	[132]
	DBD	He/Ethylene	Biosensors	[142]
Collagen	Custom-built	He	Polystyrene labware	[140]
	Custom-built	He	Wound treatment	[141]
Elastin	DBD	He, N_2/Lactic acid solution	Bioactive biodegradable surfaces	[139]
Laccase	Atmospheric pressure plasma jet	He	Biocoatings, biosensors	[135–137]
Lipase	DBD	He/Ethylene	Protein immobilization	[138]
Lysozyme	DBD	He/Ethylene	Drug delivery	[134]
	DBD		Protein immobilization	[143]

recently been of great interest to the scientific community due to its biogenic origin, biocompatibility in application and biodegradability.

Pistillo et al. deposited **L-lactic acid** at reduced pressure in a radio frequency discharge by sublimating the precursor at 110°C, with plasma power from 2 to 150 W and deposition times of 2–80 min. Plasma power was the key parameter influencing the chemical structure, as shown by previously mentioned studies. Successful deposition of COOH-rich coatings at low plasma power that were stable in water showed the material's potential for use as a platform for cell cultures.[144]

Another method, plasma-assisted vapor thermal deposition (PAVTD) was used by Krtous et al. for depositing thin films from **poly(lactic acid)** (PLA). A polymer is used as a precursor and heated at reduced pressure to its chain decomposition temperature. The resulting species are then activated and fragmented by a plasma initiating polymerization. PAVTD is considered to yield polymers with properties intermediate between those of a conventional polymer and those of a plasma polymer obtained by PECVD. In agreement with studies already mentioned, it was found for PLA that the structural integrity of the precursor decreases with increasing deposition power, as films deposited at higher plasma powers showed a decreased oxygen and increased methyl and ether group content. The average amount of intact PLA chain units was up to 4 for films deposited at low powers. At increasing powers, the PLA unit chain length decreases down to almost monomeric lactic acid units that are statistically separated by CH_3/CH_2 or ether groups. The resulting polymer network can be described as a statistical block-copolymer network from PLA, hydrocarbon units, and poly(ethylene-oxide)-like units, which confirms the ability of PAVTD to combine both characteristics of conventional polymerization and PECVD.[145] Plasma polymerized poly(lactic acid) coatings further showed controlled drug release properties and biodegradability, making the material highly interesting as a platform for biomedical devices. The drug release was studied using nisin, an antibacterial peptide, showing a clear relationship with the discharge power. At low powers, nisin passed through micro-scale pores, and drug release was delayed for hours or days, while at high powers, the drug was released within minutes through buckling instabilities. Bactericidal activities against *M. luteus* correlated with the observed drug release kinetics.[146]

Ligot et al. found that plasma power has the greatest influence among plasma deposition parameters on **ethyl lactate** plasma polymers deposited at reduced pressure. XPS and chemical derivatization experiments showed that higher power leads to increased fragmentation of the precursor and a consequential decrease in COOX functionalities. At the same time, ToF-SIMS and mechanical profilometry demonstrated a higher degree of crosslinking for polymers deposited under these conditions. Tuning the degree of crosslinking, the water/gas diffusion rate and the amount of ester bonds via controlling the plasma parameters shows the potential to enable the precise design of (bio)degradable barrier coatings.[147] Moreover, films with a higher degree of crosslinking show improved mechanical properties such as hardness, viscoelastic recovery (i.e., self-healing ability), creep, wear, and fracture resistance since plastic contributions (e.g., viscoplasticity) decrease.[148] In addition, the ester content within the plasma phase was examined by combining residual gas analysis mass

spectroscopy with in situ FTIR spectroscopy and Density Functional Theory calculations. It was shown that an increase in plasma power generally leads to a decrease in ester species in both the plasma and the resulting polymer.[149]

Furthermore, Nisol et al. investigated the energetic parameters of atmospheric PECVD of ethyl lactate in a DBD reactor. Plasma polymers with energies per molecule ranging from 21 to 42 eV/molecule and varying amounts of ester functionalities and crosslinking were observed. The degradation rate of these polymers in aqueous media could likewise be predicted from employed flow rates and resulting energies per molecule.[150]

The influence of the carrier gas on the resulting plasma polymer was shown by Laurent et al. in a study on plasma polymerized ethyl lactate deposited in an atmospheric pressure dielectric barrier discharge using either N_2 or Ar as carrier gas. They found that polymers deposited with N_2 carrier gas mainly contain isolated hydrophilic functionalities leading to fast degradation in aqueous environments. Polymers deposited with Ar carrier gas not only degrade more slowly, corresponding more closely to the behavior of conventional lactide-based polymers, but additionally show a greater structural retention of the ethyl lactate precursor and are mainly composed of a hydrocarbon structure containing comparably low amounts of ester moieties.[151]

Different dielectric barrier discharge modes at atmospheric pressure have been examined by Milaniak et al., who compared the deposition characteristics of ethyl lactate in PECVD in the glow and filamentary dielectric barrier discharge using FTIR spectroscopy. The degree of polymerization, homogeneity, and competition between deposition and etching depend on the discharge mode. The deposition further depends on bond dissociation energies and fragment stability, as stable fragments and bonds with high dissociation energies are best preserved.[152]

Overall, the precise inquiry into the process of plasma polymerization of lactic acid derivatives may lead toward new functional polymers with both tunable ester content and biodegradability.

3 | CONCLUSION AND FUTURE CHALLENGES

Plasma polymer coatings derived from natural precursors show exciting potential for application in biomedicine, organic electronics, packaging, and many more areas. Fundamental research has proven basic applicability and properties in laboratory conditions and at small scales. However, for real-life use, process adaption to industrial scales remains a challenge, as many devices still operate at low pressures or can only treat small areas. To make use of PECVD's low chemical consumption, molecules need sufficient volatility for easy transfer into the gas phase, which greatly restricts the precursor choice. For biomedical applications, further insight into compatibility with human organisms is required, while for packaging solutions, biodegradability and barrier properties need to be explored in more detail. At the same time, model substrates must be replaced by scaffolds relevant to applications, which is often challenging due to manifold interactions between substrates and plasma. Further, to date results obtained by plasma polymerization strongly depend on the choice of plasma device and can hardly be considered universally applicable. Better chemically defined deposition could be achieved by combining plasma polymerization by techniques suitable for separation into single molecules such as electrospraying. While proof of concept experiments focusing on applications have been performed, there is still little insight into the actual processes occurring in the plasma phase and during the polymerization process. The influence of individual plasma parameters, precursor functionality, and polymerization mechanisms are poorly understood and polymer structural characterization remains an unsolved challenge. Gas phase analysis and structural elucidation combining conventional or inventing new analytical methods therefore is imperative to understanding structure–property relationships and to selecting the most suitable precursors with respect to the desired applications. In-depth examination of the auto-oxidation process and the resulting matter of long-term consistency of physicochemical properties additionally needs to be conducted. In the field of biogenic precursors, these challenges are intensified by the natural variance in the already complex material composition and properties. Nonetheless, biogenic precursors remain of indispensable importance for replacing non-regenerative, fossil-based resources. Ultimately, low material consumption of plasma deposition is a key factor in the implementation of sustainable, green chemistry processes. Plasma polymerization of biogenic precursors can therefore be expected to play a leading part in future coating applications.

AUTHOR CONTRIBUTIONS

Amelia Loesch-Zhang was involved in investigation and writing—original draft. Amelia Loesch-Zhang and Andreas Geissler were involved in conceptualization. All authors were involved in writing—reviewing and editing. Andreas Geissler and Markus Biesalski were involved in supervision.

ACKNOWLEDGMENTS

This study was funded as part of the BioPlas4Paper project by Agency for Renewable Resources (Fachagentur Nachwachsende Rohstoffe e.V.—FNR), grant number 2220HV017A. The authors would like to thank Martin Bellmann, Dennis Marvin Janek Moeck, and Joern Appelt for fruitful discussions. Open Access funding enabled and organized by Projekt DEAL.

CONFLICT OF INTEREST STATEMENT

The authors declare no conflict of interest.

DATA AVAILABILITY STATEMENT

Not applicable.

ORCID

Andreas Geissler http://orcid.org/0000-0002-4284-7942

REFERENCES

[1] L. Tonks, *Am. J. Phys.* **1967**, *35*, 857.
[2] R. Jafari, S. Asadollahi, M. Farzaneh, *Plasma Chem. Plasma Process.* **2013**, *33*, 177.
[3] U. Stroth, *Plasmaphysik*, Springer, Berlin, Heidelberg, **2018**.
[4] A. Fridman, A. Chirokov, A. Gutsol, *J. Phys. D Appl. Phys.* **2005**, *38*, R1.
[5] H. Conrads, M. Schmidt, *Plasma Sources Sci. Technol.* **2000**, *9*, 441.
[6] F. Dene, *Prog. Polym. Sci.* **2004**, *29*, 815.
[7] C. Tendero, C. Tixier, P. Tristant, J. Desmaison, P. Leprince, *Spectrochim. Acta Part B* **2006**, *61*, 2.
[8] (a) A. Rutscher, H. Deutsch, *Plasmatechnik. Grundlagen und Anwendungen; eine Einführung*, Hanser, München **1984**; (b) N. S. J. Braithwaite, *Plasma Sources Sci. Technol.* **2000**, *9*, 517.
[9] H. V. Boenig, *Plasma Sci. Technol.*, **1982**, 16.
[10] B. Eliasson, U. Kogelschatz, *IEEE Trans. Plasma Sci.* **1991**, *19*, 1063.
[11] L. Bárdos, H. Baránková, *Thin Solid Films* **2010**, *518*, 6705.
[12] A. A. Fridman, *Plasma Chemistry*, Cambridge University Press, Cambridge, **2012**.
[13] U. Kogelschatz, *Plasma Phys. Control. Fusion* **2004**, *46*, B63.
[14] A. Bogaerts, E. Neyts, R. Gijbels, J. van der Mullen, *Spectrochim. Acta Part B* **2002**, *57*, 609.
[15] W. Siemens, *Annalen der Physik und Chemie* **1857**, *178*, 66.
[16] U. Kogelschatz, *IEEE Trans. Plasma Sci.* **2002**, *30*, 1400.
[17] U. Kogelschatz, *Contrib. Plasma Phys.* **2007**, *47*, 80.
[18] U. Kogelschatz, *Plasma Chem. Plasma Process.* **2003**, *23*, 1.
[19] B. Eliasson, U. Kogelschatz, *IEEE Trans. Plasma Sci.* **1991**, *19*, 309.
[20] M. Laroussi, T. Akan, *Plasma Process. Polym.* **2007**, *4*, 777.
[21] A. Schutze, J. Y. Jeong, S. E. Babayan, P. Jaeyoung Park, G. S. Selwyn, R. F. Hicks, *IEEE Trans. Plasma Sci.* **1998**, *26*, 1685.
[22] D. D. Pappas, *J. Vac. Sci. Technol. A* **2011**, *29*, 20801.
[23] D. Merche, N. Vandencasteele, F. Reniers, *Thin Solid Films* **2012**, *520*, 4219.
[24] H. Kakiuchi, H. Ohmi, K. Yasutake, *J. Vac. Sci. Technol. A* **2014**, *32*, 30801.
[25] F. Massines, C. Sarra-Bournet, F. Fanelli, N. Naudé, N. Gherardi, *Plasma Process. Polym.* **2012**, *9*, 1041.
[26] J. Y. Jeong, S. E. Babayan, V. J. Tu, J. Park, I. Henins, R. F. Hicks, G. S. Selwyn, *Plasma Sources Sci. Technol.* **1998**, *7*, 282.
[27] O. V. Penkov, M. Khadem, W.-S. Lim, D.-E. Kim, *J. Coat. Technol. Res.* **2015**, *12*, 225.
[28] (a) S. Förster, C. Mohr, W. Viöl, *Surf. Coat. Technol.* **2005**, *200*, 827; (b) H. Koinuma, H. Ohkubo, T. Hashimoto, K. Inomata, T. Shiraishi, A. Miyanaga, S. Hayashi, *Appl. Phys. Lett*. **1992**, *60*, 816; (c) M. Laroussi, X. Lu, *Appl. Phys. Lett*. **2005**, *87*, 113902; (d) C. Cheng, Z. Liye, R.-J. Zhan, *Surface Coat. Technol*. **2006**, *200*, 6659.
[29] M. Bellmann, C. Ochs, M. Harms, W. Viöl, *DE102016209097A1*, **2016**.
[30] (a) S. Bekeschus, P. Favia, E. Robert, T. von Woedtke, *Plasma Process. Polym.* **2019**, *16*, 1800033; (b) R. Brandenburg, A. Bogaerts, W. Bongers, A. Fridman, G. Fridman, B. R. Locke, V. Miller, S. Reuter, M. Schiorlin, T. Verreycken, K. Ostrikov, *Plasma Process. Polym*. **2019**, *16*, 1700238; (c) U. Cvelbar, J. L. Walsh, M. Černák, H. W. de Vries, S. Reuter, T. Belmonte, C. Corbella, C. Miron, N. Hojnik, A. Jurov, H. Puliyalil, M. Gorjanc, S. Portal, R. Laurita, V. Colombo, J. Schäfer, A. Nikiforov, M. Modic, O. Kylian, M. Polak, C. Labay, J. M. Canal, C. Canal, M. Gherardi, K. Bazaka, P. Sonar, K. K. Ostrikov, D. Cameron, S. Thomas, K. Weltmann, *Plasma Process. Polym*. **2019**, *16*, 1700228; (d) M. Šimek, M. Černák, O. Kylián, R. Foest, D. Hegemann, R. Martini, *Plasma Process. Polym*. **2019**, *16*, 1700250.
[31] R. d'Agostino, P. Favia, C. Oehr, M. R. Wertheimer, *Plasma Process. Polym.* **2005**, *2*, 7.
[32] E. M. Liston, L. Martinu, M. R. Wertheimer, *J. Adhes. Sci. Technol.* **1993**, *7*, 1091.
[33] (a) A. Holländer, R. Wilken, J. Behnisch, *Surf. Coat. Technol.* **1999**, *116-119*, 788; (b) J. Katz, S. Gershman, A. Belkind, *Plasma Med*. **2015**, *5*, 223.
[34] P. Chu, *Mater. Sci. Eng. R Rep*. **2002**, *36*, 143.
[35] (a) D. Mariotti, A. C. Bose, K. Ostrikov, *IEEE Trans. Plasma Sci.* **2009**, *37*, 1027; (b) H. Puliyalil, U. Cvelbar, *Nanomaterials*, **2016**, *6*, 108.
[36] (a) A. Vesel, M. Mozetic, *J. Phys. D Appl. Phys.* **2017**, *50*, 293001; (b) J. M. Grace, L. J. Gerenser, *J Dispers. Sci. Technol*. **2003**, *24*, 304; (c) C.-M. Chan, T.-M. Ko, H. Hiraoka, *Surf. Sci. Reports*. **1996**, *24*, 1.
[37] T. Desmet, R. Morent, N. de Geyter, C. Leys, E. Schacht, P. Dubruel, *Biomacromolecules* **2009**, *10*, 2351.
[38] (a) K. Schröder, A. Meyer-Plath, D. Keller, W. Besch, G. Babucke, A. Ohl, *Contrib. Plasma Phys.* **2001**, *41*, 562; (b) J. Friedrich, *Rev. Adhes. Adhes*. **2018**, *6*, 253.
[39] (a) S.-H. Gao, M.-K. Lei, Y. Liu, L.-S. Wen, *Appl. Surf. Sci.* **2009**, *255*, 6017; (b) R. Barni, C. Riccardi, E. Selli, M. R. Massafra, B. Marcandalli, F. Orsini, G. Poletti, L. Meda, *Plasma Process. Polym*. **2005**, *2*, 64; (c) M. R. Sanchis, V. Blanes, M. Blanes, D. Garcia, R. Balart, *Eur. Polym. J.* **2006**, *42*, 1558.

[40] K. Bazaka, M. V. Jacob, R. J. Crawford, E. P. Ivanova, *Acta Biomater.* **2011**, *7*, 2015.
[41] Y. Ferreira da Silva, V. M. Queiroz, I. C. S. Kling, B. S. Archanjo, R. N. Oliveira, R. A. Simao, *Plasma Process. Polym.* **2020**, *17*, 2000035.
[42] (a) M.-C. Popescu, M. Totolin, C. M. Tibirna, A. Sdrobis, T. Stevanovic, C. Vasile, *Int. J. Biol. Macromol.* **2011**, *48*, 326; (b) L. Cabrales, N. Abidi, *Appl. Surf. Sci*. **2012**, *258*, 4636.
[43] S. Sousa, C. Gaiolas, A. P. Costa, C. Baptista, M. E. Amaral, *Cell. Chem. Technol.* **2016**, *50*, 711.
[44] C. Gaiolas, M. N. Belgacem, L. Silva, W. Thielemans, A. P. Costa, M. Nunes, M. J. Santos Silva, *J. Colloid Interface Sci.* **2009**, *330*, 298.
[45] H. Biederman, *Plasma Polymer Films*, Imperial College Press, London, **2004**.
[46] G. S. Schoepfle, L. H. Connell, *Indust. Eng. Chem.* **1929**, *21*, 529.
[47] E. G. Linder, A. P. Davis, *J. Phys. Chem.* **1931**, *35*, 3649.
[48] (a) H. König, G. Helwig, *Zeitschrift for Physik*. **1951**, *129*, 491-503; (b) R. H. Hansen, H. Schonhorn, *J. Polym. Sci. Part B Polym. Lett.* **1966**, *4*, 203; (c) T. Willliams, M. W. Hayes, *Nature* **1966**, *209*, 769; (d) A. R. Denaro, P. A. Owens, A. Crawshaw, *Eur. Polym. J*. **1968**, *4*, 93; (e) A. R. Westwood, *Eur. Pol. J.* **1971**, *7*, 363; (f) H. Yasuda, *J. Polym. Sci., Part D Macromol. Rev.* **1981**, *16*, 199; (g) H. Kobayashi, A. T. Bell, M. Shen, *Macromolecules* **1974**, *7*, 277.
[49] J. Goodman, *J. Polym. Sci.* **1960**, *44*, 551.
[50] A. Bradley, J. P. Hammes, *J. Electrochem. Soc.* **1963**, *110*, 15.
[51] K. Jesch, J. E. Bloor, P. L. Kronick, *J. Polym. Sci., Part A-1 Polym. Chem.* **1966**, *4*, 1487.
[52] H. Yasuda, T. Hsu, *J. Polym. Sci. Polym. Chem. Ed.* **1977**, *15*, 81.
[53] J. Mertens, J. Baneton, A. Ozkan, E. Pospisilova, B. Nysten, A. Delcorte, F. Reniers, *Thin Solid Films* **2019**, *671*, 64.
[54] J. Mertens, B. Nisol, J. Hubert, F. Reniers, *Plasma Process. Polym.* **2020**, *17*, 1900250.
[55] K. Bazaka, M. V. Jacob, B. F. Bowden, *J. Mater. Res.* **2011**, *26*, 1018.
[56] H. Yasuda, T. Hirotsu, *J. Polym. Sci. Polym. Chem. Ed.* **1978**, *16*, 743.
[57] (a) B. Nisol, S. Watson, S. Lerouge, M. R. Wertheimer, *Plasma Process. Polym.* **2016**, *13*, 900; (b) A. Kakaroglou, B. Nisol, K. Baert, I. de Graeve, F. Reniers, G. van Assche, H. Terryn, *RSC Adv*. **2015**, *5*, 27449.
[58] (a) H. Yasuda, C. E. Lamaze, *J. Appl. Polym. Sci.* **1973**, *17*, 1519; (b) H. Yasuda, C. E. Lamaze, *J. Appl. Polym. Sci*. **1973**, *17*, 1533.
[59] H. Yasuda, M. O. Bumgarner, J. J. Hillman, *J. Appl. Polym. Sci.* **1975**, *19*, 531.
[60] F. Huang, L. Chen, H. Wang, Z. Yan, *Chem. Eng. J.* **2010**, *162*, 250.
[61] (a) A. Batan, B. Nisol, A. Kakaroglou, I. de Graeve, G. van Assche, B. van Mele, H. Terryn, F. Reniers, *Plasma Process. Polym.* **2013**, *10*, 857; (b) B. Nisol, G. Arnoult, T. Bieber, A. Kakaroglou, I. de Graeve, G. van Assche, H. Terryn, F. Reniers, *Plasma Process. Polym*. **2014**, *11*, 335.
[62] J. Friedrich, *Plasma Process. Polym.* **2011**, *8*, 783.
[63] (a) B. Nisol, S. Watson, S. Lerouge, M. R. Wertheimer, *Plasma Process. Polym.* **2016**, *13*, 557; (b) B. Nisol, S. Watson, S. Lerouge, M. R. Wertheimer, *Plasma Process. Polym*. **2017**, *14*, 1600191; (c) B. Nisol, S. Watson, A. Meunier, D. Juncker, S. Lerouge, M. R. Wertheimer, *Plasma Process. Polym*. **2018**, *15*, 1700132.
[64] (a) M. Moreno-Couranjou, J. Guillot, J.-N. Audinot, J. Bour, E. Prouvé, M.-C. Durrieu, P. Choquet, C. Detrembleur, *Plasma Process. Polym.* **2020**, *17*, 1900187; (b) G. P. Lopez, B. D. Ratner, *Langmuir* **1991**, *7*, 766; (c) F. Hilt, D. Duday, N. Gherardi, G. Frache, J. Didierjean, P. Choquet, *RSC Adv*. **2015**, *5*, 4277.
[65] N. D. Boscher, F. Hilt, D. Duday, G. Frache, T. Fouquet, P. Choquet, *Plasma Process. Polym.* **2015**, *12*, 66.
[66] C. L. Rinsch, X. Chen, V. Panchalingam, R. C. Eberhart, J. H. Wang, R. B. Timmons, *Langmuir* **1996**, *12*, 2995.
[67] (a) C. Gaiolas, A. P. Costa, M. Nunes, M. J. S. Silva, M. N. Belgacem, *Plasma Process. Polym.* **2008**, *5*, 444-452; (b) A. Grüniger, P. Rudolf von Rohr, *Surf. Coat. Technol*. **2003**, *174-175*, 1043.
[68] S. E. Alexandrov, M. L. Hitchman, *Chem. Vap. Deposition* **2005**, *11*, 457.
[69] T. Belmonte, G. Henrion, T. Gries, *J. Therm. Spray Technol.* **2011**, *20*, 744.
[70] R. A. Wolf, *Atmospheric Pressure Plasma for Surface Modification*, John Wiley & Sons, Hoboken, N.J, **2013**.
[71] (a) Y. Sawada, S. Ogawa, M. Kogoma, *J. Phys. D Appl. Phys.* **1995**, *28*, 1661; (b) K. Schmidt-Szalowski, Z. Rżanek-Boroch, J. Sentek, Z. Rymuza, Z. Kusznierewicz, M. Misiak, *Plasma Polym*. **2000**, *5*, 173; (c) M. C. Kim, C.-P. Klages, *Surf. Coat. Technol*. **2009**, *204*, 428.
[72] (a) I. Vinogradov, A. Lunk, *Plasma Process. Polym.* **2005**, *2*, 201; (b) R. Prat, Y.J. Koh, Y. Babukutty, M. Kogoma, S. Okazaki, M. Kodama, *Polymer* **2000**, *41*, 7355.
[73] H.-R. Lee, D. Kim, K.-H. Lee, *Surf. Coat. Technol.* **2001**, *142-144*, 468.
[74] A. Shah, S. Patel, E. Narumi, D. T. Shaw, *Appl. Phys. Lett.* **1990**, *57*, 1452.
[75] B. Nisol, C. Poleunis, P. Bertrand, F. Reniers, *Plasma Process. Polym.* **2010**, *7*, 715.
[76] G. Da Ponte, E. Sardella, F. Fanelli, A. van Hoeck, R. d'Agostino, S. Paulussen, P. Favia, *Surf. Coat. Technol.* **2011**, *205*, 525.
[77] (a) M. C. Vasudev, K. D. Anderson, T. J. Bunning, V. V. Tsukruk, R. R. Naik, *ACS Appl. Mater. Interfaces* **2013**, *5*, 3983; (b) G. Ozaydin-Ince, A. M. Coclite, K. K. Gleason, *Rep. Prog. Phys.* **2012**, *75*, 016501; (c) S. Bhatt, J. Pulpytel, F. Arefi-Khonsari, *Surf. Innovat.* **2015**, *3*, 63; (d) J. Ibrahim, S. A. Al-Bataineh, A. Michelmore, J. D. Whittle, *Plasma Chem. Plasma Proces* **2021**, *41*, 47; (e) K. Vasilev, S. S. Griesser, H. J. Griesser, *Plasma Process. Polym*. **2011**, *8*, 1010; (f) F. Fanelli, *Surface Coat. Technol*. **2010**, *205*, 1536; (g) F. F. Shi, *Surface Coat. Technol*. **1996**, *82*, 1.
[78] F. Bakkali, S. Averbeck, D. Averbeck, M. Idaomar, *Food Chem. Toxicol.* **2008**, *46*, 446.
[79] S. Burt, *Int. J. Food Microbiol.* **2004**, *94*, 223.
[80] F. Nazzaro, F. Fratianni, R. Coppola, V. D. Feo, *Pharmaceuticals* **2017**, *10*, 86.
[81] D. Sakthi Kumar, M. G. Krishna Pillai, *Thin Solid Films* **1999**, *353*, 249.

[82] D. Sakthi Kumar, K. Nakamura, S. Nishiyama, H. Noguchi, S. Ishii, K. Kashiwagi, Y. Yoshida, *J. Appl. Polym. Sci.* **2003**, *90*, 1102.

[83] M. V. Jacob, C. D. Easton, G. S. Woods, C. C. Berndt, *Thin Solid Films* **2008**, *516*, 3884.

[84] C. D. Easton, M. V. Jacob, R. A. Shanks, B. F. Bowden, *Chem. Vap. Deposit.* **2009**, *15*, 179.

[85] C. D. Easton, M. V. Jacob, *Thin Solid Films* **2009**, *517*, 4402.

[86] C. D. Easton, M. V. Jacob, *J. Appl. Polym. Sci.* **2010**, *115*, 404.

[87] C. D. Easton, M. V. Jacob, *Polym. Degrad. Stab.* **2009**, *94*, 597.

[88] A. Al-Jumaili, K. Bazaka, M. Jacob, *Nanomaterials* **2017**, *7*, 270.

[89] A. Al-Jumaili, S. Alancherry, K. Bazaka, M. Jacob, *Electronics* **2017**, *6*, 86.

[90] B. E. Hennekam, S. A. Al-Bataineh, A. Michelmore, *J. Appl. Polym. Sci.* **2020**, *137*, 49288.

[91] B. Mol, J. James, C. Joseph, M. R. Anantharaman, M. J. Bushiri, *SN Appl. Sci.* **2020**, *2*, 801.

[92] O. Bazaka, K. Prasad, I. Levchenko, M. V. Jacob, K. Bazaka, P. Kingshott, R. J. Crawford, E. P. Ivanova, *Molecules* **2021**, *26*, 7133.

[93] M. V. Jacob, R. S. Rawat, B. Ouyang, K. Bazaka, D. S. Kumar, D. Taguchi, M. Iwamoto, R. Neupane, O. K. Varghese, *Nano Lett.* **2015**, *15*, 5702.

[94] J. Romo-Rico, S. Murali Krishna, J. Golledge, A. Hayles, K. Vasilev, M. V. Jacob, *Plasma. Process. Polym.* **2022**, *19*, 2100220.

[95] B. Mol, J. James, K. K. Anoop, I. Sulaniya, C. Joseph, M. R. Anantharaman, M. J. Bushiri, *J. Mater. Sci. Mater. Electron.* **2019**, *30*, 12603.

[96] S. Alancherry, K. Bazaka, M. V. Jacob, *J. Polym. Environ.* **2018**, *26*, 2925.

[97] D. S. Grant, J. Ahmed, J. D. Whittle, A. Michelmore, K. Vasilev, K. Bazaka, M. V. Jacob, *Molecules* **2021**, *26*, 4762.

[98] K. Bazaka, M. V. Jacob, *Mater. Lett.* **2009**, *63*, 1594.

[99] A. Kumar, D. S. Grant, K. Bazaka, M. V. Jacob, *J. Appl. Polym. Sci.* **2018**, *135*, 45771.

[100] K. Bazaka, M. V. Jacob, *Polym. Degrad. Stab.* **2010**, *95*, 1123.

[101] K. Bazaka, M. Jacob, V. K. Truong, R. J. Crawford, E. P. Ivanova, *Polymers* **2011**, *3*, 388.

[102] A. Kumar, S. Mills, K. Bazaka, N. Bajema, I. Atkinson, M. V. Jacob, *Surf. Coat. Technol.* **2018**, *349*, 426.

[103] M. V. Jacob, K. Bazaka, M. Weis, D. Taguchi, T. Manaka, M. Iwamoto, *Thin Solid Films* **2010**, *518*, 6123.

[104] M. V. Jacob, K. Bazaka, D. Taguchi, T. Manaka, M. Iwamoto, *Chem. Phys. Lett.* **2012**, *528*, 26.

[105] A. Kumar, A. Al-Jumaili, K. Prasad, K. Bazaka, P. Mulvey, J. Warner, M. V. Jacob, *Plasma Chem. Plasma Process.* **2020**, *40*, 339.

[106] J. Ahmad, K. Bazaka, J. D. Whittle, A. Michelmore, M. V. Jacob, *Plasma Process. Polym.* **2015**, *12*, 1085.

[107] K. Bazaka, J. Ahmad, M. Oelgemöller, A. Uddin, M. V. Jacob, *Sci. Rep.* **2017**, *7*, 45599.

[108] T. G. Getnet, G. F. da Silva, I. S Duarte, M. E. Kayama, E. C. Rangel, N. C. Cruz, *Materials* **2020**, *13*, 3166.

[109] T. G. Getnet, M. E. Kayama, E. C. Rangel, I. C. S. Duarte, G. F. da Silva, N. C. Cruz, *J. Mater. Res. Technol.* **2022**, *18*, 2217.

[110] A. Pegalajar-Jurado, C. D. Easton, K. E. Styan, S. L. McArthur, *J. Mater. Chem. B* **2014**, *2*, 4993.

[111] M. N. Mann, E. R. Fisher, *ACS Appl. Mater. Interfaces* **2017**, *9*, 36548.

[112] Y. W. Chan, K. S. Siow, P. Y. Ng, U. Gires, B. Yeop Majlis, *Mater. Sci. Eng. C* **2016**, *68*, 861.

[113] S. Tone, T. Masawaki, K. Eguchi, *J. Membr. Sci.* **1996**, *118*, 31.

[114] M. Gürsoy, *J. Appl. Polym. Sci.* **2021**, *138*, 49722.

[115] M. V. Jacob, N. S. Olsen, L. J. Anderson, K. Bazaka, R. A. Shanks, *Thin Solid Films* **2013**, *546*, 167.

[116] K. Bazaka, R. Destefani, M. V. Jacob, *Sci. Rep.* **2016**, *6*, 38571.

[117] D. Gerchman, B. Bones, M. B. Pereira, A. S. Takimi, *Prog. Org. Coat.* **2019**, *129*, 133.

[118] L. J. Anderson, M. V. Jacob, *Appl. Surf. Sci.* **2010**, *256*, 3293.

[119] C. D. Easton, M. V. Jacob, R. A. Shanks, *Polymer* **2009**, *50*, 3465.

[120] M. V. Jacob, C. D. Easton, L. J. Anderson, K. Bazaka, *Int. J. Modern Phys. Conf. Ser.* **2014**, *32*, 1460319.

[121] K. Bazaka, M. V. Jacob, R. A. Shanks, *Adv. Mater. Res.* **2010**, *123-125*, 323.

[122] (a) L. J. Anderson, M. V. Jacob, *Mater. Sci. Eng. B*. **2012**, *177*, 311; (b) L. J. Anderson, M. V. Jacob, *Thin Solid Films* **2013**, *534*, 452.

[123] K. Bazaka, M. V. Jacob, *J. Mater. Res.* **2011**, *26*, 2952.

[124] (a) J. Ahmad, K. Bazaka, M. Jacob, *Electronics* **2014**, *3*, 266; (b) J. Ahmad, K. Bazaka, M. Oelgemöller, M. Jacob, *Coatings* **2014**, *4*, 527; (c) I. Ahmad, M. I. Khan, H. Khan, M. Ishaq, R. Tariq, K. Gul, W. Ahmad *J. Appl. Polym. Sci.* **2015**, *132*, 42318.

[125] (a) T. G. Getnet, M. E. Kayama, E. C. Rangel, N. C. Cruz, *Polymers* **2020**, *12*, 2692; (b) T. G. Getnet, M. E. Kayama, E. C. Rangel, I. C. S. Duarte, G. F. da Silva, N. C. Cruz, *Thin Solid Films* **2021**, *734*, 138833.

[126] (a) I. Sugimoto, M. Nakamura, H. Kuwano, *Anal. Chem.* **1994**, *66*, 4316; (b) I. Sugimoto, M. Nakamura, H. Kuwano, *Sens. Actuat. Chem* **1996**, *36*, 342; (c) M. Seyama, Y. Iwasaki, S. Ogawa, I. Sugimoto, A. Tate, O. Niwa, *Analyt. Chem.* **2005**, *77*, 4228.

[127] K. D. Anderson, J. M. Slocik, M. E. McConney, J. O. Enlow, R. Jakubiak, T. J. Bunning, R. R. Naik, V. V. Tsukruk, *Small* **2009**, *5*, 741.

[128] K. D. Anderson, S. L. Young, H. Jiang, R. Jakubiak, T. J. Bunning, R. R. Naik, V. V. Tsukruk, *Langmuir* **2012**, *28*, 1833.

[129] K. D. Anderson, K. Marczewski, S. Singamaneni, J. M. Slocik, R. Jakubiak, R. R. Naik, T. J. Bunning, V. V. Tsukruk, *ACS Appl. Mater. Interfaces* **2010**, *2*, 2269.

[130] P. Heyse, R. Dams, S. Paulussen, K. Houthoofd, K. Janssen, P. A. Jacobs, B. F. Sels, *Plasma Process. Polym.* **2007**, *4*, 145.

[131] P. Heyse, A. van Hoeck, M. B. J. Roeffaers, J.-P. Raffin, A. Steinbüchel, T. Stöveken, J. Lammertyn, P. Verboven, P. A. Jacobs, J. Hofkens, S. Paulussen, B. F. Sels, *Plasma Process. Polym.* **2011**, *8*, 965.

[132] P. Heyse, M. B. J. Roeffaers, S. Paulussen, J. Hofkens, P. A. Jacobs, B. F. Sels, *Plasma Process. Polym.* **2008**, *5*, 186.

[133] M. G. Ortore, R. Sinibaldi, P. Heyse, S. Paulussen, S. Bernstorff, B. Sels, P. Mariani, F. Rustichelli, F. Spinozzi, *Appl. Surf. Sci.* **2008**, *254*, 5557.
[134] F. Palumbo, G. Camporeale, Y.-W. Yang, J.-S. Wu, E. Sardella, G. Dilecce, C. D. Calvano, L. Quintieri, L. Caputo, F. Baruzzi, P. Favia, *Plasma Process. Polym.* **2015**, *12*, 1302.
[135] S. Malinowski, P. Herbert, J. Rogalski, J. Jaroszyńska-Wolińska, *Polymers* **2018**, *10*, 532.
[136] S. Malinowski, C. Wardak, J. Jaroszyńska-Wolińska, P. Herbert, R. Panek, *Sensors* **2018**, *18*, 4086.
[137] S. Malinowski, J. Jaroszyńska-Wolińska, P. A. F. Herbert, *J. Mater. Sci.* **2019**, *54*, 10746.
[138] Y.-C. Cheng, C.-P. Hsiao, Y.-H. Liu, C.-H. Yang, C.-Y. Chiang, T.-R. Lin, Y.-W. Yang, J.-S. Wu, *Plasma Process. Polym.* **2018**, *15*, 1700173.
[139] G. Da Ponte, E. Sardella, F. Fanelli, S. Paulussen, P. Favia, *Plasma Process. Polym.* **2014**, *11*, 345.
[140] D. O'Sullivan, H. McArdle, J.-A. O'Reilly, R. J. O'Kennedy, R. Forster, L. O'Neill, *Plasma Process. Polym.* **2020**, *17*, 1900147.
[141] L. O'Neill, P. Dobbyn, M. Kulkarni, A. Pandit, *Clin. Plama Med.* **2018**, *12*, 23.
[142] D. Liu, T. He, Z. Liu, S. Wang, Z. Liu, M. Rong, M. G. Kong, *Plasma Process. Polym.* **2018**, *15*, 1870022.
[143] C.-P. Hsiao, C.-C. Wu, Y.-H. Liu, Y.-W. Yang, Y.-C. Cheng, F. Palumbo, G. Camporeale, P. Favia, J.-S. Wu, *IEEE Trans. Plasma Sci.* **2016**, *44*, 3091.
[144] B. R. Pistillo, L. Detomaso, E. Sardella, P. Favia, R. d'Agostino, *Plasma Process. Polym.* **2007**, *4*, S817.
[145] Z. Krtouš, L. Hanyková, I. Krakovský, D. Nikitin, P. Pleskunov, O. Kylián, J. Sedlaříková, J. Kousal, *Materials* **2021**, *14*, 459.
[146] Z. Krtouš, J. Kousal, J. Sedlaříková, Z. Kolářová Rašková, L. Kučerová, I. Krakovský, J. Kučera, S. Ali-Ogly, P. Pleskunov, A. Choukourov, *Surf. Coat. Technol.* **2021**, *421*, 127402.
[147] S. Ligot, F. Renaux, L. Denis, D. Cossement, N. Nuns, P. Dubois, R. Snyders, *Plasma Process. Polym.* **2013**, *10*, 999.
[148] S. Ligot, E. Bousser, D. Cossement, J. Klemberg-Sapieha, P. Viville, P. Dubois, R. Snyders, *Plasma Process. Polym.* **2015**, *12*, 508.
[149] S. Ligot, M. Guillaume, P. Raynaud, D. Thiry, V. Lemaur, T. Silva, N. Britun, J. Cornil, P. Dubois, R. Snyders, *Plasma Process. Polym.* **2015**, *12*, 405.
[150] B. Nisol, S. Watson, S. Lerouge, M. R. Wertheimer, *Plasma Process. Polym.* **2016**, *13*, 965.
[151] M. Laurent, J. Koehler, G. Sabbatier, C. A. Hoesli, N. Gherardi, G. Laroche, *Plasma Process. Polym.* **2016**, *13*, 711.
[152] N. Milaniak, G. Laroche, F. Massines, *Plasma Process. Polym.* **2021**, *18*, 2000248.

How to cite this article: A. Loesch-Zhang, A. Geissler, M. Biesalski, *Plasma Process Polym.* **2023**;*20*:e2300016.
https://doi.org/10.1002/ppap.202300016